AALTO UNIVERSITY
SCHOOL OF ELECTRICAL ENGINEERING
Department of Communications and Networking (ComNet)

Effect of Feedback Delay in Cooperative Multipoint Communications

Pradeep Mallya

A thesis submitted in partial fulfillment of the requirements for the degree of Master of Science in Technology.

Helsinki, February 20, 2013

Supervisor: Prof. Jyri Hämäläinen

Instructor: Dr. Alexis Dowhuszko

AALTO UNIVERSITY
SCHOOL OF ELECTRICAL ENGINEERING

ABSTRACT OF THE
MASTER'S THESIS

Author:	Pradeep Mallya
Name of the Thesis:	Effect of Feedback Delay in Cooperative Multipoint Communications
Date:	February 20, 2013 **Number of pages:** 72
Department:	Department of Communications and Networking
Professorship:	S-72
Supervisor:	Jyri Hämäläinen, Professor, D.Sc
Instructor:	Alexis Dowhuszko, D.Sc

There has been an enormous growth in the field of wireless communications, but the demands for higher data rates and better capacity have never decreased. With the link throughputs approaching the Shannon limit, several techniques are now focussing on improving the Signal-to-Interference-plus-Noise power Ratio (SINR) to further improve the system performance.

The SINR at the cell edge is generally low, and the users at the cell edge are the most sensitive to interference. Improving the SINR at the cell edge results in better throughput, coverage and capacity. One method to achieve this is by using cooperative transmissions from the different base stations in the vicinity of the mobile station. The cooperation relies on the channel feedback provided by the mobile station. Although this method is very effective, there may be feedback delays which degrade the system performance.

The objective of this Thesis is to study the effect of feedback delay in cooperative multipoint communication systems. To achieve this goal, the different feedback techniques are analyzed, and the most optimum method is selected based on the channel conditions, user profile and the expected feedback delay. The performance of several hierarchical feedback schemes are also analyzed, and an opportunistic feedback method is conceptualized as a conclusion of this Thesis.

Keywords: Cooperative communications, Channel state information, Feedback delay, Multicell processing, Rayleigh channels, Signal to noise ratio, Time-varying channels.

Acknowledgements

This Thesis would not be complete without the guidance and support of several individuals, who, in one way or the other, have left a lasting impression on me and have influenced my approach during the preparation and completion of this study.

It gives me immense pleasure to acknowledge the support and help of my supervisor, Prof. Jyri Hämäläinen. It has been a pleasure working with his research group. His knowledge and passion for the subject has been an inspiration to me.

I express my sincere thanks to my instructor, Dr. Alexis Dowhuszko, whose dedication, perseverance and outstanding intelligence had made me look up to him as my role model. I cannot thank him enough for the amount of care he has taken in going through this Thesis. His attention to detail has always amazed me. I have learnt so much from him, and will remember his advices for the rest of my life.

I am always indebted to my parents, my sister and my closest friends for being there to help me stay focussed and motivated. Life in Finland would have been cold and dark without their support and encouragement.

Finally, I would like to dedicate this Thesis to my grandma, who has given me so much love and affection, and who left this world a day before I was selected for this research work.

Otaniemi, February 20, 2013

Pradeep Mallya

Contents

List of Abbreviations

1G	First Generation
2G	Second Generation
3G	Third Generation
3GPP	Third Generation Partnership Project
4G	Fourth Generation
AWGN	Additive White Gaussian Noise
BEP	Bit Error Probability
BEP	Bit Error Rate
BPSK	Binary Phase Shift Keying
BS	Base Station
CDF	Cumulative Distribution Function
CoMP	Coordinated Multi-Point
CQI	Channel Quality Indicator
CS/CB	Coordinated Scheduling/Beamforming
CSI	Channel State Information
CTP	Cooperative Transmission Point
FDD	Frequency-Division Duplexing

HCC	Hierarchical Cophasing-Cophasing
HCS	Hierarchical Cophasing-Selection
ISI	Inter-Symbol Interference
LTE	Long Term Evolution
MIMO	Multiple-Input Multiple-Output
MISO	Multiple-Input Single-Output
MRC	Maximum Ratio Combining
MS	Mobile Station
OFDM	Orthogonal Frequency Division Multiplexing
P2P	Point-to-Point Communications
PDF	Probability Density Function
PDSCH	Physical Downlink Shared Channel
PMI	Precoding Matrix Indicator
RI	Rank Indicator
RRH	Remote Radio Head
SINR	Signal-to-Interference-plus-Noise power Ratio
SIMO	Single-Input Multiple-Output
SISO	Single-Input Single-Output
SNR	Signal-to-Noise power Ratio
STBC	Space Time Block Coding
STTD	Space Time Transmit Diversity
TAS	Transmit Antenna Selection

TBF	Transmit Beamforming
UMTS	Universal Mobile Telecommunications System
UTRAN	Universal Terrestrial Radio Access Network
WCDMA	Wideband Code Division Multiple Access

List of Notations

a	Amplitude of the transmitted BPSK signal
B_d	Doppler Spread
D	Feedback delay
d	Distance
$\mathbb{E}\langle\rangle$	Mathematical expectation of a variable
$\mathbb{E}\{\|r\|^2\}$	Total received power
$e()$	Modulation error rate
f_c	Carrier frequency
f_d	Doppler Frequency
f_m	Maximum Doppler frequency
$g()$	Complex envelope in Jakes' model
$g_I()$	In-phase component of the complex envelope
$g_Q()$	Quadrature phase component of the complex envelope
γ	Signal-to-Interference power Ratio
$\mathbb{E}\langle\gamma\rangle$	Signal-to-Noise power Ratio gain
h	Channel gain vector
$J_k(\cdot)$	Bessel function of the first kind and k-th order

λ	Wavelength of the wireless signal
M	Number of transmit antennas
n	Instantaneous channel noise
N_{fb}	Number of feedback bits
N_0	Power spectral density of noise
N_s	Number of sinusoids used in Jakes' model
$p_X()$	Probability density function of random variable X
P_e	Bit Error Probability
$Q()$	Q-function
r	Received signal
$S()$	Power spectral density
σ_X^2	Variance of random variable X
T_c	Coherence time of a wireless channel
T_d	Delay spread of a wireless channel
T_s	Time slot duration
τ	Feedback delay
t_i	Propagation time on the i^{th} slot
Υ	Mean power in case of power imbalance
v	Receiver velocity
w	Transmit weight
$\hat{w}$	Optimum value of transmit weight
$\mathcal{W}$	Quantization set of transmit weights

W_c	Coherence bandwidth of a wireless channel
x	Input signal
y	Channel output signal
$(\cdot)^*$	Complex conjugate of a complex number

List of Figures

List of Tables

Chapter 1

Introduction

The first chapter gives a background to the research work that has been undertaken. The research problem, as well as contributions of this Thesis are described briefly. The different sections of this chapter aim to give to the reader a perspective on the scope of the work conducted. The final section contains the outline of the structure of this Thesis.

1.1 Background

Wireless communication systems are evolving continuously. There have been rapid advancements in the technology since its inception, from the time first generation (1G) systems were introduced in the 1980s, to the tremendous success of second generation (2G) systems and the growing popularity of the third generation (3G) networks. The technologies are becoming better to cater to the needs of the customers.

However, the demands of the customers have also been growing with the advancements in technology. A 1000 fold increase in traffic from today is expected by the year 2020 [1] with over 50 billion connected wireless devices [2]. The networks have to be ready to cope up with this increase. The fourth generation (4G) networks are now getting deployed, and they are touted to be the future networks. Tremendous amount of research work is also being conducted

on this technology. Several techniques and concepts are being developed to enhance the bandwidth efficiency and improve the capacity of the networks.

One such approach to enhance the system capacity is to use universal frequency reuse [3] [4], where the entire bandwidth is used for the transmission of the data. In these systems, the same spectrum is used in every cell.

The use of the same bandwidth by the adjacent cells results in adjacent cell interference. This severely affects the cell edge users, as they typically experience low Signal-to-Interference-plus-Noise power Ratios (SINRs). One method that can be used for preventing the problem of low throughput at the cell edge is by cooperation between the transmitting entities. The interference to users in the adjacent cell can be minimized, and the SINR can be maximized by coordinated transmissions. The transmissions are coordinated based on several open-loop or closed-loop techniques. In a closed-loop system, the channel state information (CSI) is made available at the transmitter from the feedback sent by the receiver. These coordination techniques are referred to as *cooperative multipoint transmission* or *multicell cooperation* [5]. Cooperative multipoint transmission has been researched upon, and standardized in 3rd generation partnership project (3GPP) specifications as coordinated multipoint (CoMP). In CoMP, several transmitting base stations (BSs) cooperate with each other to minimize the interference at the mobile station (MS). There are several methods used in multicell cooperation systems, with different transmission and feedback techniques.

As the advantages of cooperative multipoint transmission systems are numerous, several studies are being conducted on its potential features and characteristics. Many new proposals and methods are being investigated, but very few studies take into account the effect of feedback delay. In practice, wireless channels undergo fading processes that are continuous in nature, and there is always temporal correlation between the samples. However, in most studies, approximate channel models (like block Rayleigh fading channel models) are considered. In these channel models, the samples are assumed to be uncorrelated and constant during its coherence time. Unfortunately, block fading

channel models cannot be used to study the performance of the system in case of feedback delay.

In this Thesis, a more realistic, continuously varying correlated channel is built using Clarke's model. This channel is then used to study the impact of delay on the system. A closed-loop system with a single receiver and multiple transmitters is considered, where the receiver continuously sends feedback to the transmitters informing about the channel conditions. Several procedures are carried out on the signals at the transmitters, based on the channel conditions estimated using the feedback. The behaviour of the system changes in the presence of feedback delay, and the system performance expectedly comes down with increasing mobile speed. This demands further study of the characteristics of the system with feedback delay. The research problem arises due to the presence of delay, and it can be clearly defined as shown in the next section.

1.2 Research Problem and Methodology

Several methods can be used for cooperative multipoint transmission. It is possible to choose the optimum transmit method depending on the channel parameters and user characteristics, but the metrics to select the optimum method has not been clearly defined. The performance of these different methods have not yet been studied very well in the presence of delay.

The main objective of this Thesis is to study the effect of feedback delay in cooperative multipoint communication systems, in order to develop opportunistic feedback mechanisms that enable better performance. This is achieved by finding the analytical relations to assess the performance, developing a simulator to implement the various closed-loop transmit-diversity techniques, and demonstrating the performance of the system in the presence of delays. To achieve this goal, several intermediate steps were defined:

1. The first and the foremost requirement was to build a channel simulator using Jakes' model, to simulate a wireless channel that is close to a

practical channel with correlation between the samples.

2. The different transmit diversity techniques needed to be studied and simulated, and the simulated performance was to be compared to the analytically derived relations.

3. The different methods needed to be studied for the different values of power imbalance and delays, for different number of transmit antennas, and for various feedback resolutions.

1.3 Contributions of the Thesis

As mentioned in the previous section, the performance of cooperative multipoint communication systems have not been studied very well in the case of feedback delay. This Thesis presents the study about the effect of feedback delay in a multicell cooperation system. Depending on the performance of the various multicell cooperation techniques in different conditions, the most efficient method could be chosen. The Thesis also studies the performance of system at different power imbalance situations, occurring when the receiving terminal is at different distances from the cooperating base stations. By analyzing the performance of the system in different environments, an opportunistic feedback method can be conceptualized to optimize the performance of the system.

The previous studies on various closed-loop transmit-diversity techniques [6] [7] have been extended to include more scenarios, and the performance of these methods have been simulated and compared to the analytical derivations. An overview of the structure of the Thesis is given in the next section, and it shows the sequence of steps that are presented to coherently answer the research problems defined in the previous section.

1.4 Outline of the Thesis

The structure of the Thesis is the following:
Chapter 2 starts with an introduction to mobile communications. It describes the basic form of point-to-point communications, and then describes multiple-input multiple-output (MIMO) systems. The different types of cooperative multipoint communications systems and its analogy to the 3GPP standardized feature of CoMP is also discussed.
Chapter 3 describes briefly the various models that have been considered while building the simulator for the channel. Knowledge of the simulator assists in understanding the various characteristics of the obtained results, and helps to understand the conclusions.
Chapter 4 describes the transmit-diversity techniques that are used for cooperative multipoint communication systems.
Chapter 5 discusses the performance of the different cooperative multipoint systems that are considered in this study. This chapter forms the most important part of the work, as the analytical derivations as well as its comparison to the simulated values are described in detail.
Chapter 6 provides an overview of the hierarchical feedback methods that are considered in this Thesis. Their performance in the case of delay is also shown based on numerical simulation results.
Finally, Chapter 7 gives the conclusions of the Thesis, and then describes the scope for further improvements and future research in this area.

Chapter 2

Cooperative Multipoint Communications

The aim of this chapter is to introduce multi-antenna communication system concepts. The chapter is intended to give a general overview of the different techniques used for wireless communications, and the advantages of each of these over the others. In addition, this chapter provides details of cooperative multipoint communication concepts.

2.1 Introduction to Multi-Antenna Techniques

Over the course of the evolution of communication systems, several antenna diversity techniques have been used based on the data rates needed, and the complexity of the system. The simplest system is the single-input single-output (SISO) system. This system consists of a single transmitting antenna, and a single receiving antenna as shown in Fig. 2.1a. Single-input single-output has no spatial diversity and, therefore, does not need extra processing. Understandably, these systems have limited performance. Since there is no spatial diversity, the interference and fading in the channel would severely affect the system. The throughput and channel capacity is limited by the

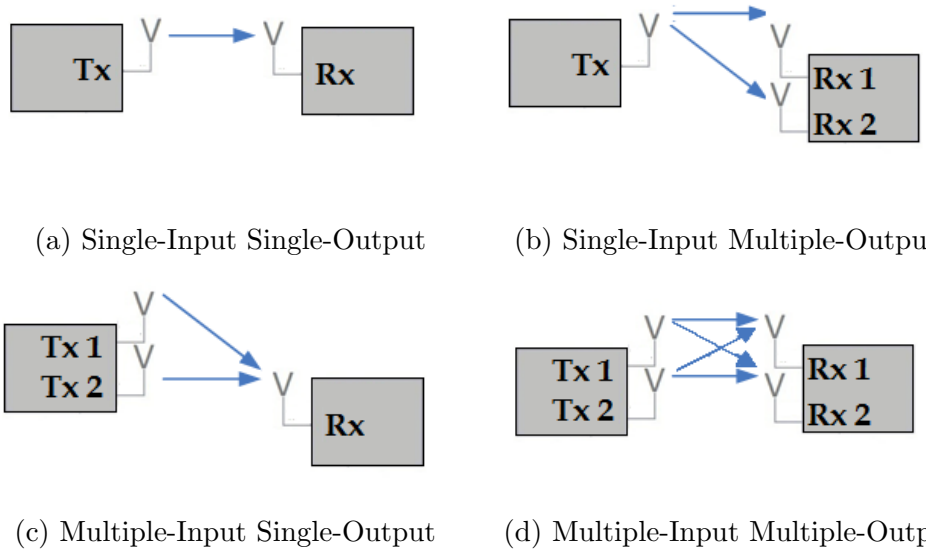

(a) Single-Input Single-Output (b) Single-Input Multiple-Output

(c) Multiple-Input Single-Output (d) Multiple-Input Multiple-Output

Figure 2.1: Illustration of antenna diversity techniques. The input and output refers to the number of transmitters and receivers, respectively.

signal-to-noise power ratio (SNR) according to Shannon's law:

$$C = W \cdot \log_2(1 + \text{SNR}) \tag{2.1}$$

where C is the channel capacity and W is the communication bandwidth.

Another multi-antenna technique that can be considered is the single-input multiple-output (SIMO) system, which has a single transmitting antenna and multiple receive antennas as shown in Fig. 2.1b. The main advantage of this system over SISO is in fading environments. In these environments, the receiver can process the signals received in its multiple antennas, and maximize the received power using techniques like maximum ratio combining (MRC).
Multiple-input single-output (MISO) system is shown in Fig. 2.1c. In this system, there are multiple transmitters and a single receiver. The transmitter with the best signal quality is chosen, or several transmitted signals are combined to maximize the signal power at the receiver side.
If several transmit and receive antennas are used, the receiving antennas can choose the best transmitted signal based on some predefined algorithms, and

the performance of the system can be enhanced. This is the idea behind multiple-input multiple-output (MIMO) systems. Fig. 2.1d shows a simple schematic diagram of a MIMO System. Coding is used on the channels to separate the signals in the different streams and to prevent interference. The channel throughput can be increased tremendously using MIMO.
However, the presence of multiple antennas at the transmitter as well as receiver increase the implementation complexity, and require additional processing power. The use of MIMO is not very advantageous when there are system constraints on size or complexity. In such cases, MISO systems are considered. Here, the processing is moved from the receiver to the transmitter, and this is a significant advantage if the transmitters can have high processing capabilities, like in a base station of a cellular system.

In a MISO system, the total SINR of the system can be improved if the different transmitting antennas coordinate transmissions, such that the receiver gets maximum SINR. This forms the basis for cooperative multipoint transmission, also referred to as multicell coordination.

2.2 Cooperative Multipoint Transmission

Cooperative multipoint transmission or multicell cooperation [5] is considered as a method to increase the cell-edge throughput and improve the coverage of the cell, subsequently enhancing the system throughput [8] [9]. It is basically a distributed MISO system, where the user at the cell-edge can receive useful signals from multiple transmitters/base stations. In conventional systems, the signals received from the BSs other than from the serving base station would for considered interference. This results in the degradation of the overall performance. If there is coordination between the different transmitters and base stations, the interfering signal power can be minimized, and in some cases, utilized as a useful signal. These coordinating transmitting antennas or base stations are referred to as the cooperative transmitter set, and the individual transmitters are referred to as cooperative transmitting points (CTP). The

coordination between these transmitting points can be simple, as in the techniques used to avoid interference by beamforming, or can be more complex, where the same data is transmitted by the different points, after application of transmit weights, so that they are received with a high SINR.

Multicell cooperation can be used in both, uplink and downlink. In the uplink, several geographically separated base stations can receive the uplink data from the same user. This may involve multicell reception or interference coordination decisions among the different cells to reduce interference. Multicell cooperation in uplink does not have as big impact as in downlink, and the remainder of this Thesis mainly concentrates on downlink multicell cooperation. The considered cooperation approaches are interference coordination and multicell processing.

2.2.1 Interference Coordination

In interference coordination, only the serving cell contains the data to be transmitted, but beamforming decisions and scheduling of the users are done in coordination with the different CTPs in the cooperative transmitter set. This method is mainly used to reduce the interference of the signals from the adjacent cells by using beamforming, with the non-serving cells redirecting their beams away from the receiver whenever possible, to minimize the interference. In highly loaded cells, the beamforming matrices are jointly decided by the CTPs, using the CSI feedback of the MS, to reduce interference [10] [11]. In 3GPP standard terminology, interference coordination is usually referred to as coordinated scheduling/beamforming (CS/CB). From its first proposal [12], CS/CB has been performed by assigning a CTP to a cluster of users. The MS are clustered depending on their profiles and channel conditions. The CTPs know the instances at which they need to transmit to a particular user assigned to it. The SINR and the throughput of the system is therefore maximized by the optimum scheduling of the users.

Figure 2.2 shows the general structure of an interference coordination system.

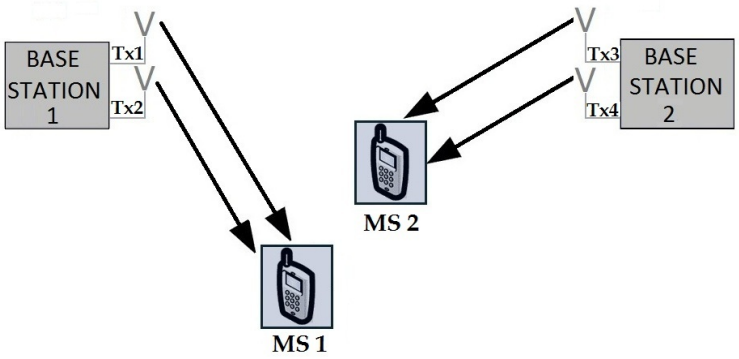

Figure 2.2: Interference coordination in a cooperative multipoint transmission system. The black solid lines indicate the downlink transmission from the BS to its respective MS.

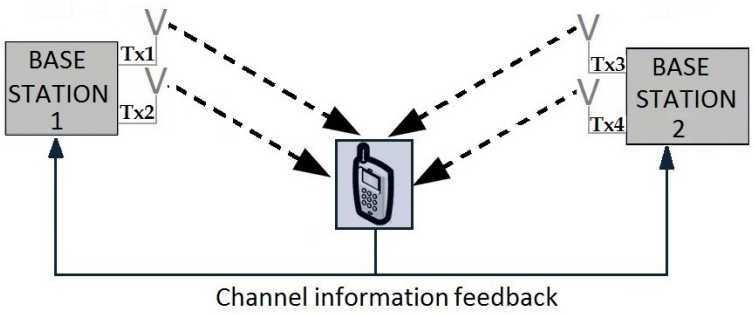

Figure 2.3: Multicell processing in a cooperative multipoint transmission system. The black dashed lines indicate that the data to be transmitted is present at all the transmitters of the cooperative transmitter set, and any transmitter could be used for transmission.

2.2.2 Multicell Processing

In this category of multicell cooperation, the physical downlink shared channel (PDSCH) data is available at all the points of the cooperating transmitter set. Based on the channel conditions and user parameters like speed of the common mobile station, it is decided if the receiver is sent data from a single transmitter or from multiple transmitters in the cooperating set. A general overview of multicell processing is shown in the Fig. 2.3.

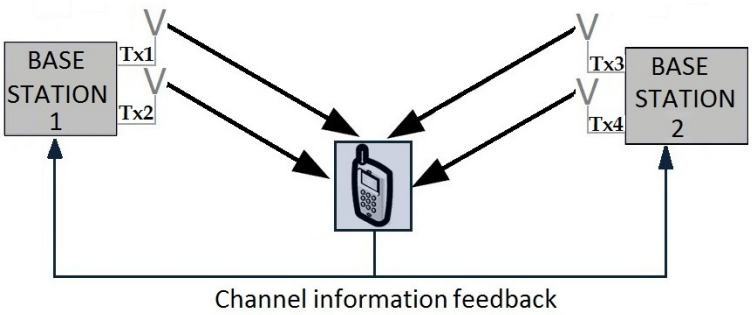

Figure 2.4: Joint transmission in multicell processing. The solid lines indicate the transmission of the data. Multiple transmitters transmit data simultaneously to the common mobile station.

Multicell processing can be very advantageous in cell edge situations, where the interfering signals can be converted to the desired signal. Multicell processing consists of two methods:

1. Joint transmission, and
2. Dynamic cell selection.

Joint Transmission

In this method, the data is sent simultaneously to the receiver from multiple points of the cooperative transmitter set as shown in Fig. 2.4. The entire set or a subset of the cooperative set can be used for the simultaneous transmission.

Dynamic Cell Selection

In this method, the receiver gets the PDSCH data from only one point in the cooperative transmitter set as shown in Fig. 2.5. Several metrics, like the channel characteristics and location of the user, can be used to choose the transmitting point. The other points in the set are continuously monitored, and they also contain the data that is being transmitted. In every subframe, the transmission points are selected to ensure efficient transmission with the best SINR.

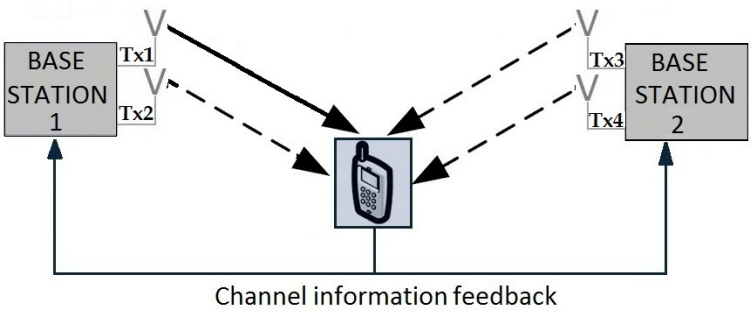

Figure 2.5: An example of dynamic cell selection in multicell processing. The solid lines indicate the transmission of the data and the dashed lines indicate those transmitters that contain data but are not transmitting in that subframe.

One or more of the above categories can be used simultaneously in a system to form a hybrid category. In this Thesis, the different hybrid categories among multicell processing are considered. Using these techniques, several scenarios can be covered in homogeneous and heterogeneous networks. Models of this Thesis can also be considered in the following scenarios that are defined by the 3GPP standards [9]:

1. The first scenario is in a homogeneous macrocell network, where multicell cooperation is applied between the sectors of the same base station. There is no need for a separate interface as the coordination is inter-BS.

2. The second scenario is also in a homogeneous macrocell network, with a base station present with several low powered remote radio heads (RRH). The coordination is done between the different cells in the macro network.

3. The third scenario is in the heterogeneous network case. In this scenario, a macrocell and several low powered cells with its own unique identity is present inside the macrocell. These low powered microcells/picocells coordinate with the high powered macrocell in different scenarios of powers, and distances of the common receiver from the BS.

4. The fourth scenario is also related to a heterogeneous networks. Here, low power cells that form the distributed antenna system, are present

inside the macrocell coverage. These low power cells have the same cell ID as the macrocell.

Although the scenarios mentioned above involve the use of both multicell processing and interference coordination, this Thesis mainly focusses on the method of multicell processing. Schemes are developed for interference mitigation between the different streams of data transmitted by the various CTPs. This is required as data with random powers or phases would cause interference, and the system performance would degrade. These methods are called transmit beamforming (TBF) [13], and they are described in the Chapter 4.

Chapter 3

System Model

In this chapter, the general system model is explained and the definition of the various terms and assumptions in the system and the simulator are discussed in detail. This chapter also gives a brief explanation about the simulator model that is used.

3.1 Feedback Delay in a System

The main goal of this Thesis is to study the performance of a closed-loop cooperative multi-antenna transmission system in the presence of delay. The system considered is assumed to be frequency-division duplexed (FDD), with a channel of one frequency used for uplink transmission, and another frequency used for the downlink. The uplink and downlink channels consist of frames of data, and these frames are again divided into slots. Although this system can be considered as in the standardized Universal Mobile Telecommunications System (UMTS) or a Long Term Evolution (LTE) system, this Thesis considers a generic model that is not bound by the specifications. A simple figure illustrating the slot structure in a generic FDD system is shown in Fig. 3.1. It is assumed that there is no transmission delay.

In the downlink transmission frame, there are usually pilot signals that are transmitted at the beginning of the slot. These signals are also known as the

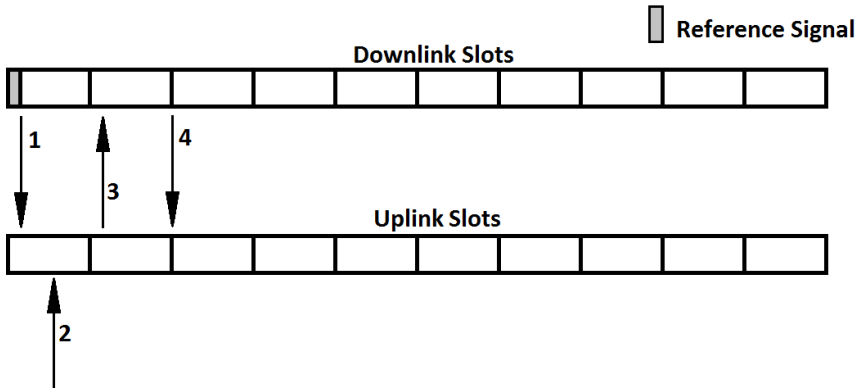

Figure 3.1: Example of 2 slot delay. The downlink and uplink slots of a generic FDD system are shown. 1: Downlink transmission from BS to MS. 2: Feedback message generated by MS using reference signals for channel estimation. 3: Feedback transmitted to BS on uplink. 4: Transmit weights applied by BS based on the feedback.

reference signals. Reference signals are known physical layer signals which can be used by the MS to estimate the downlink power. The reference signals can be user specific or cell specific, and can be used either for tracking [14] or to estimate the channel either directly or by interpolation [15] across several instances. In the case of closed-loop systems, these reference signals are the only possible entities that can be used to estimate the channel and generate the CSI. In the Fig. 3.1, the x-axis represents time, and the different numbered labels indicate the following:

1. The downlink transmission from the BS to the MS takes place with the transmission of the reference signal. This signal is needed by the MS to estimate the channel and to generate the feedback message.

2. The transmitted reference signal is now processed by the MS to estimate the channel. The delay present here is the processing delay of the MS.

3. The feedback message is now sent to the BS in the uplink control channel. The number of feedback bits on the uplink is usually limited, and therefore, the size of the feedback sent in the uplink is small.

4. The BS, after reception of the CSI from the MS, calculates the weights that have to be used for transmit beamforming, and then sends the trans-

mission to the user based on the feedback.

Hence, the channel condition at the beginning of the first slot is used for the transmit weight calculation in the third slot, resulting in a delay of 2 slots. The slot durations can vary, depending on the system that is being used. In UMTS, the slot length is equal to 2ms, and in LTE, refers to a duration of 1ms. The channel conditions would be different at the different instances, and it is necessary to study the performance of the system in the presence of delay.

3.2 Delay Spread and Coherence Bandwidth

A vital parameter in wireless systems with multipath propagation is the delay spread (T_d). It can be considered as the time difference between the arrival of the signals on the shortest path and the longest path [16]. It can be represented by the equation:

$$T_d = \max_{i,j} |t_i - t_j|, \tag{3.1}$$

where t_i and t_j are the propagation times on the i^{th} and j^{th} path, respectively. Delay spread is usually very small in the case of microcells, and is in the range of a few microseconds. It needs to be taken into account only when the cell sizes are large. The value of delay spread determines the coherence of the channel in frequency domain.

It is important to know the variation of the wireless channel with frequency. We now arrive at a term called the coherence bandwidth (W_c), which refers to the bandwidth in which the wireless channel remains constant. Coherence bandwidth is inversely proportional to the delay spread, T_d, and is related as follows:

$$W_c = \frac{1}{(2T_d)}. \tag{3.2}$$

If the bandwidth of the input signal is less than the coherence bandwidth, then the fading is uniform irrespective of the frequency. These wireless channels are called *flat fading channels*. In these channels, the delay experienced by the different paths are smaller than the symbol duration. Hence, a single

tap channel model is sufficient to represent the entire signal.
In this Thesis, a frequency flat Rayleigh channel is considered in the analysis.

3.3 Coherence Time and Doppler Spread

The variation of the mobile channel with respect to the relative motion of the transmitter or receiver can be clearly identified by using the coherence time and the Doppler spread. When there is a relative motion between the transmitter and receiver, the received signal frequency will be different from the transmitted signal frequency, and this difference is known as the Doppler frequency (f_d). Doppler frequency can be calculated using the relation

$$f_d = \frac{v}{\lambda} \cos\theta = f_m \cos\theta, \tag{3.3}$$

where v [ms^{-1}] is the relative velocity between the transmitter and the receiver, λ [m] is the wavelength of the signal, and θ is the angle between the transmitter's forward velocity and the line-of-sight from the receiver.

The largest difference between the Doppler shifts, i.e.,

$$B_d = \max_{i,j} |f_d(i) - f_d(j)|, \tag{3.4}$$

is called the Doppler spread (B_d), and this maximum is taken over all the paths that has a significant contribution to the power. Doppler spread is the range of frequencies over which the Doppler spectrum is non-zero. Doppler spread can, therefore, be visualized as the spectral broadening that is caused by the change of the channel with time, due to the relative motion between the transmitter and MS.

Coherence time can be considered as the time domain equivalent of the coherence bandwidth. It defines the time varying nature of the frequency dispersion in the wireless channel. If the symbol duration is larger than the coherence time of the channel, the channel will change during the duration of the symbol

transmission, and the received signal will be distorted. The coherence time (T_c) is inversely related to the Doppler frequency of the channel, i.e,

$$T_c = \frac{1}{f_d}. \tag{3.5}$$

If two symbols arrive at the receiver with a time difference greater than the coherence time of the wireless channel, then these 2 symbols would be affected differently by this channel. Conversely, the time over which the transmitted signals have high probability of being correlated is the coherence time. Considering 2 signals, and assuming that the correlation between the signals is above 50%, the relation for coherence time is then given [17] as

$$T_c = \frac{9}{16\pi f_d}. \tag{3.6}$$

The value of the coherence time can be considered as the geometric mean of (3.5) and (3.6), and can be expressed as

$$T_c = \sqrt{\frac{9}{16\pi f_d^2}}. \tag{3.7}$$

If the coherence time of the wireless channel is smaller than the feedback delay, then the channel can be considered as a fast fading channel [16]. Otherwise, the channel is slow fading. In this Thesis, the delay caused by the feedback is considered to be much smaller than the coherence time of the channel, roughly speaking, about 10%-20% of T_c.

3.4 Clarke's Model

In this Thesis, a frequency-flat fading channel is considered. The simulation of the flat fading channel is done using a popular statistical model, known as the Clarke's model [18] [19]. A practical wireless channel, when there is a relative motion between the transmitter and the receiver, with no direct line-of-sight between them is considered. In this system, the received signal is mainly com-

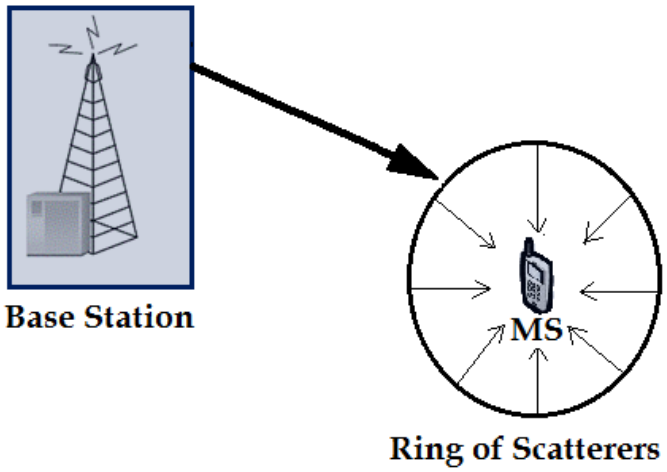

Figure 3.2: Clarke's one ring model. The scatterers in the environment are assumed to be homogeneously distributed, at equal distances from the mobile station (i.e., like in a ring)

posed of the scattered signals and diffracted signals from different obstacles. The channels can be simulated by assuming that the received signal is a sum of several horizontal plane waves, with random angles of arrival and random phases distributed in the interval $[-\pi,+\pi)$. A model that is used for this purpose is as shown in Fig. 3.2. The scatterers are assumed to be homogeneously distributed around the receiver, at equal distances from the receiver, like in a ring.

With the assumption that the receiving antenna is an omnidirectional antenna, the probability density function (PDF) for the different angles of arrival α is given in [20] as

$$p_\alpha = \begin{cases} \frac{1}{2\pi} & \alpha \in [-\pi, +\pi), \\ 0 & \text{otherwise.} \end{cases}$$

Then, it is possible to define the PDF of the Doppler frequency, f_d, as follows:

$$p_F(f_d) = \begin{cases} \frac{\lambda}{\pi\, v \sqrt{1-(f\,\lambda/v)^2}} & |f_d| \leq v/\lambda, \\ 0 & |f_d| > v/\lambda. \end{cases}$$

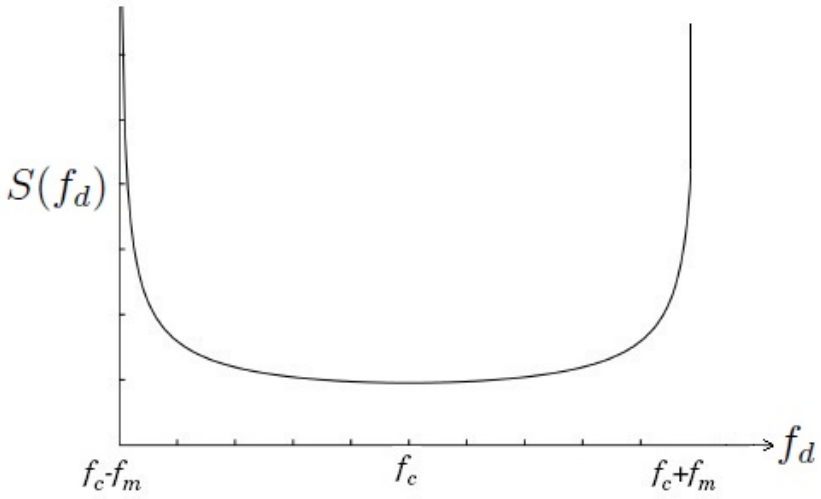

Figure 3.3: Doppler Power Spectrum in Clarke's model [20]

The power spectral density of the signals that are scattered can be estimated from the PDF of the Doppler frequency. The power spectrum density can be written as

$$S(f_d) = \int_{-\infty}^{+\infty} p_F(f_d) df \tag{3.8}$$

From equation (3.4), we can arrive at

$$S(f_d) = \begin{cases} \frac{2\sigma_0^2 \lambda}{\pi(v)\sqrt{1-(f\,\lambda/v)^2}} & |f_d| \leq v/\lambda, \\ 0 & |f_d| > v/\lambda, \end{cases}$$

where $2\sigma_0^2 = \int_{-\infty}^{+\infty} S(f_d) df$ is the total power of the scattered signals.
The Doppler power spectrum of the signal can be shown as in Fig. 3.3
It can also be deduced that the direction of motion of the receiver does not affect the Doppler spread when using Clarke's model. In this Thesis, Clarke's model is implemented using a proposal given by Jakes, called the "Sum of Sinusoids method", or more commonly, "Jakes' model". This method models a continuous time wireless Rayleigh flat fading channel [21].

3.5 Rayleigh Fading Models

While modelling a wireless channel, it can be assumed that in a duration of a single tap, the receiver gets a large number of reflected and scattered signals with random amplitudes. At high signal frequencies, the distances of the scatterers and reflectors are likely to be much larger than the wavelength of the signal. Hence, the phases of the different scattered and reflected signals can also be assumed to be independent and randomly distributed in the interval [0,2π].

Each path can be modelled as a circularly symmetric complex random variable. This single tap, which is the sum of such circularly symmetric random variable paths, can be modelled as a zero-mean Gaussian random variable following the central limit theorem. The gain of the l^{th} tap, written as $h_l[m]$, has a magnitude probability density given by [16] as

$$p_h(x) = \frac{2x}{\sigma_h^2} e^{\frac{-x^2}{\sigma_h^2}} \qquad x \geq 0, \tag{3.9}$$

where σ_h^2 represents the variance of the random variable h.

The squared magnitude of the l^{th} tap is given by a exponential distribution written as

$$p_h(x) = \frac{1}{\sigma_h^2} e^{\frac{-x}{\sigma_h^2}} \qquad x \geq 0. \tag{3.10}$$

This means that the magnitude of the signal will vary according to a Rayleigh distribution. The model with circularly symmetric complex random variables designed is called the Rayleigh fading model. This simple model gives a very reasonable approximation of the channel when there are a scatterers present. A block Rayleigh fading channel can be modelled by generating complex variables with real and imaginary parts, following independent normal Gaussian variables. These Rayleigh fading channels do not have correlation between the samples, but this is not the case in actual channels. In practical environments, the different samples always have correlation, and studying correlated channels is necessary in order to study the effect of delays. A correlated channel can be designed by using Jakes' model, such that the in-phase and quadrature-phase

components have a power spectral density resembling an isotropic scattering environment.

3.5.1 Jakes' Model

Jakes' model assumes that all the components arriving at the receiver will have equal strengths, to give a complex envelope of the form

$$g(t) = \sum_{n=1}^{N_s} e^{j(2\pi f_m t \cos\theta_n + \phi_n)}, \tag{3.11}$$

where N_s is the number of sinusoids, ϕ_n is the random phase of the n^{th} path and f_m is the maximum value of Doppler frequency. The isotropic scattering components are approximated by choosing N_s components uniformly distributed in angle given by

$$\theta_n = \frac{2\pi n}{N_s} \quad n = 1, 2, \cdots, N_s. \tag{3.12}$$

Equation (3.11) can be simplified as in [22] to give

$$g(t) = g_I(t) + j g_Q(t), \tag{3.13}$$

where

$$g(t) = \sqrt{2}\Bigg\{ \left[2\sum_{n=1}^{M_{osc}} \cos\beta_n \cos 2\pi f_n t + \sqrt{2}\cos\alpha \cos 2\pi f_m t \right] + j\left[2\sum_{n=1}^{M_{osc}} \sin\beta_n \cos 2\pi f_n t + \sqrt{2}\sin\alpha \cos 2\pi f_m t \right] \Bigg\}. \tag{3.14}$$

It is assumed that there are $M_{osc} = (N_s - 2)/4$ low frequency oscillators with frequencies $f_n = f_m \cos(2\pi n/N_s)$ and $n = 1, 2, .., M_{osc}$. Then, α and β_n are odd functions related to the random phase terms ϕ_n. Using the above relation, a simulator can be constructed as shown in Fig. 3.4.

The simulator, with $M_{osc} = 8$ is developed, and it is used to generate a continuous-time frequency-flat faded signal with correlation between the sam-

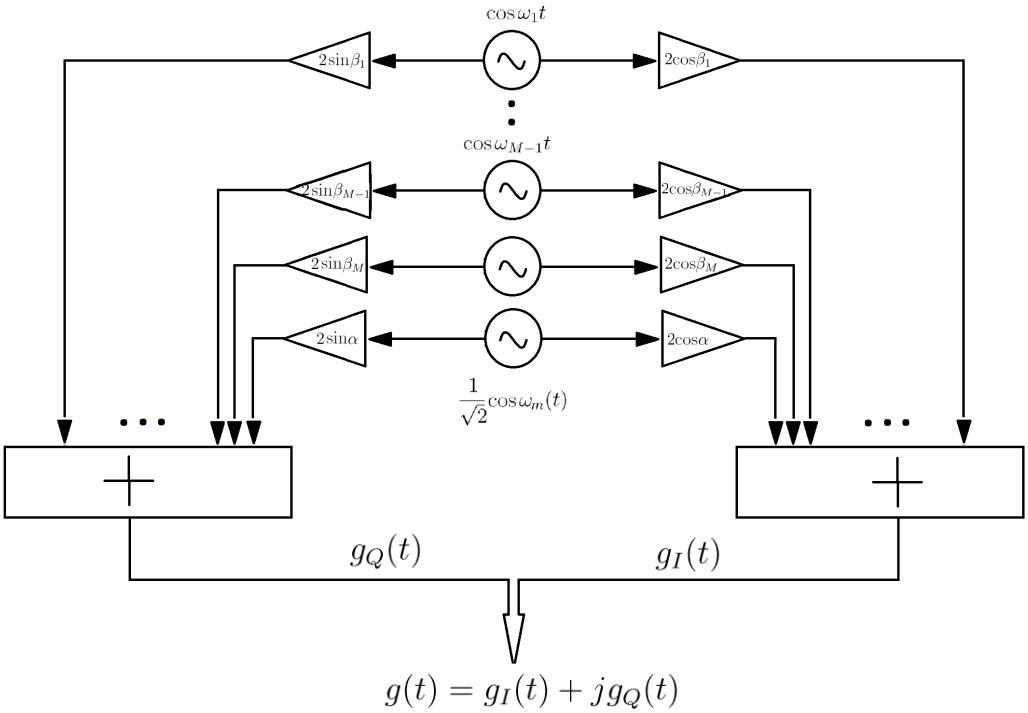

Figure 3.4: Simulator for Jakes' model [22]. A faded envelope is generated using the sum of sine methods, summing a number of low frequency oscillators.

ples. A sample of the generated waveform showing the SNR of the channel with time is as shown in Fig. 3.5.

3.6 Performance Metrics

In this section, the different performance metrics that are used in the evaluation of the performance of the different methods are discussed. The reasons for selecting these metrics are also explained briefly.

3.6.1 Bit Error Rate

Bit error rate (BER) is an effective measure to gauge the reliability of the complete system. It can be defined as the ratio of the the number of erroneous

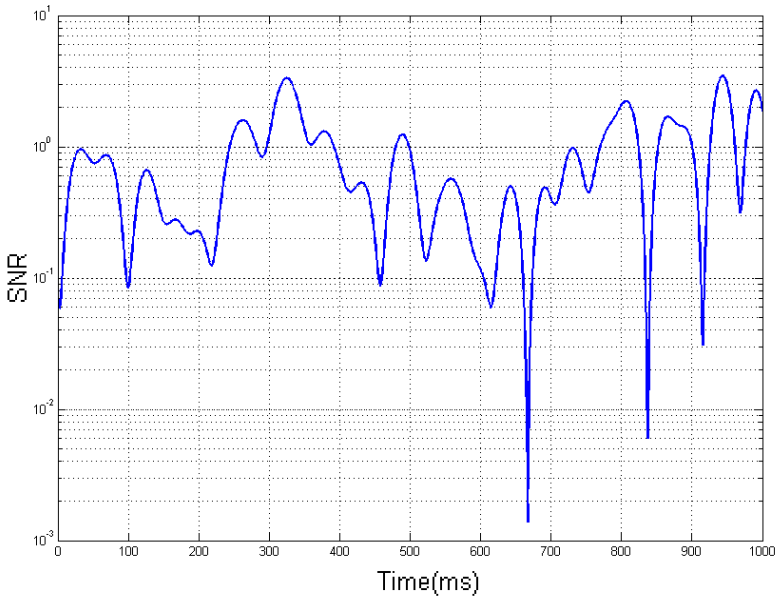

Figure 3.5: A faded signal generated using Jakes' model. Speed of the receiver is 36 km/h, carrier frequency is 2 GHz.

bits to the total number of bits transmitted. A very low bit error probability, therefore, implies that the output of the system has minimum errors. When the SINR of the system is low, and when there are channel errors, the BER may have a large value as it is affected by strong Gaussian noise present in the system.

The expected value of BER, also called the bit error probability (BEP), is another metric that is generally used. Bit error probability is calculated [23] as

$$\text{BEP} = \mathbb{E}\langle \text{BER} \rangle = \int_0^\infty p(\gamma) \cdot e(\gamma) d\gamma, \tag{3.15}$$

where $p(\gamma)$ is the PDF of SINR and $e(\gamma)$ is the error rate of modulation in terms of SINR.

When the analysis is done for transmit diversity systems with many quantization levels, the calculation of BEP becomes complex with the introduction of

several integrals, and hence obtaining a closed form expression becomes difficult. The performance of these transmit diversity systems can be studied very well using another performance metric, known as the SNR gain [23].

3.6.2 Signal-to-Noise power Ratio Gain

The SNR gain is an effective performance measure in a multi-antenna system. It is represented as $\mathbb{E}\langle\gamma\rangle$, and is the expected value of the SNR at the receiver side. It indicates the gain that is achieved because of the CSI feedback, and can be simply represented [23] as

$$\mathbb{E}\langle\gamma\rangle = \frac{\mathbb{E}\langle\gamma_{\text{CSI}}\rangle}{\mathbb{E}\langle\gamma_0\rangle}, \tag{3.16}$$

where

$$\mathbb{E}\langle\gamma_{\text{CSI}}\rangle = \mathbb{E}\left\langle \frac{P_e}{\sigma^2}|w \cdot h|^2 \right\rangle_h \tag{3.17}$$

is the expected SNR at the receiver with CSI when the weights are applied at the transmitter, and

$$\mathbb{E}\langle\gamma_0\rangle = \mathbb{E}\left\langle \frac{\text{BEP}\|h\|}{\sigma^2 M} \right\rangle, \tag{3.18}$$

represents the expected value of the received SNR in the absence of CSI feedback. $h = (h_1, h_2, \cdots, h_M)$ represents the channel gain vector, where h_1, h_2, $\cdots$, h_M represent the channel impulse response for the different streams from the M antennas.
$w = (w_1, w_2, \cdots, w_M)$ represents the transmit weights that are chosen by the transmitter depending on the feedback received from the MS. $w \in \mathcal{W}$ and $||w|| = 1$. $\mathcal{W}$ is the quantization set.

From the equations (3.17) and (3.18), it can be seen that the SNR gain will be of unitary value when there is no CSI used for the transmission. Therefore, unity represents the lower limit of this performance metric.

The next chapter gives an introduction to the methods that are used for transmit beamforming in the various diversity techniques.

Chapter 4

Transmit Diversity Techniques

In this chapter, the various transmit diversity techniques are studied, and the performance of these methods are discussed in more detail.

4.1 Introduction

Although several transmit-diversity methods have been in use for many years, it is important to first study their use in basic point-to-point communications. The disadvantages of having no diversity antennas in point-to-point communication methods justify the need for diversity, as discussed in the succeeding sections.

4.1.1 Point-to-Point Communications

The term point-to-point communications (P2P) refers to a wide variety of communication systems that also includes systems that do not use diversity techniques. The performance of these P2P systems need to be studied first, in order to understand its disadvantages, and to understand the need to develop and use diversity methods. Let us first consider a P2P system that consists of a single antenna and receiver in a Rayleigh fading channel. The filter tap is represented as a single discrete time circularly symmetric complex random variable with zero mean and unitary value of variance, written as $h \sim \mathcal{CN}(0,1)$.

Assuming coherent detection, the output during one symbol time can be written as

$$y = hx + n, \tag{4.1}$$

where $n \sim \mathcal{CN}(0, N_0/2)$ represents the noise.

For simplicity, let us assume flat fading, and consider a system which uses binary phase shift keying (BPSK) modulation with amplitude a. Therefore, the transmitted symbols $x = \pm a$. The bit error probability for a given value of h is given by

$$Q\left(\frac{a|h|}{\sqrt{N_0/2}}\right) = Q\left(\sqrt{2|h^2|\mathrm{SNR}}\right), \tag{4.2}$$

where $\mathrm{SNR} = a^2/N_0$. See [16] for more details.

The probability of error can be calculated by averaging the above Q function over the gain h. For Rayleigh fading, when $h \sim \mathcal{CN}(0,1)$ and $\mathbb{E}[|h|^2] = 1$, the integration results in

$$P_e = \mathbb{E}[Q(\sqrt{2|h|^2\mathrm{SNR}})] = \frac{1}{2}\left(1 - \sqrt{\frac{\mathrm{SNR}}{1+\mathrm{SNR}}}\right). \tag{4.3}$$

Using Taylor series, the relation can be approximated to

$$P_e \approx \frac{1}{4\mathrm{SNR}}. \tag{4.4}$$

We can see that the probability of error of a BPSK signal in a Rayleigh fading channel is very high, and the probability of error decays inversely proportional to SNR.

It can be deduced that the reliability of the communication depends only on the single communication path. The performance of the system deteriorates in the presence of channel errors. One solution to this problem is to use multiple paths for the signals. These multiple paths will undergo different, independent fading processes, and the received signal can be selected to get optimum

reception. This technique is called diversity.

4.1.2 Diversity Techniques in Communications

As analyzed in the previous section, it is advantageous to have multiple paths for the signal in the presence of errors. The attenuation in one path is compensated by the better channel condition in the other signal paths. Diversity techniques can be broadly classified in time, frequency or space (antenna), to name a few options.

Frequency Diversity

Frequency diversity is particularly applicable to combat the effects of frequency selective fading channels, where the signals with different frequencies experience different fading states. In this technique, the data to be transmitted is modulated using different frequencies, and transmitted from the same transmitter to a receiver. These signals of different frequencies are referred to as carriers.

Frequency diversity is useful in the case of wideband channels, where the transmission bandwidth is greater than the coherence bandwidth of the wireless channel. The components of the different paths can be resolved if the carriers are separated by at least a frequency band proportional to the coherence bandwidth of the channel. In this case, the different streams will undergo independent fading. At the receiver, algorithms like MRC can be used to optimally combine the different data, removing the effects of frequency selective fading.

It is clearly evident that this method uses extra bandwidth, and the achieved data rates are low. The rate cannot be increased, as sending more symbols will increase the frequency beyond the coherence bandwidth of the wireless channel. This results in inter symbol interference (ISI).

Time Diversity

Time diversity is applied in the presence of time selectivity in the fading channel. In time diversity, the signals representing the same data are sent during different times over the same wireless channel. The time intervals between the transmissions of the copies of the same signal should be greater than the coherence time of the mobile channel, so that the fading experienced by the different streams containing the same signal are independent. As a result, the fading characteristics of the channel can be considered as random. Maximum ratio combiner can also be used here to get the optimal received signal. The drawback of time diversity is the consumption of extra transmission time.

Antenna Diversity

Finally, antenna diversity technique involves the use of multiple antennas, at the receiver and/or transmitter. If the separation between the antennas is sufficiently large (generally more than half the wavelength of the signal used), the fading can be considered independent, and the diversity gain can be obtained.

Antenna diversity techniques can also be classified into receive diversity, transmit diversity and both, transmit and receive diversity simultaneously.
This Thesis considers transmit diversity, and hence, transmit diversity method and its types will be discussed in more detail in the remainder of this chapter.

4.2 Transmit Diversity

In this type of diversity, the data is transmitted simultaneously using multiple antennas. Transmit diversity can be considered as a system that mimics a controlled multipath environment. These multipath signals sum up constructively at the receiver to combat fading [24]. Downlink transmit diversity is a mandatory feature according to 3GPP specifications [25]. 3GPP specifications also define 2 modes of transmit diversity: open-loop transmit-diversity and closed-loop transmit-diversity.

Open-loop transmit-diversity is based on space-time transmit diversity (STTD), which was first proposed by Alamouti [26]. It employs space-time block coding (STBC), so that the signals are kept orthogonal.
Let us assume a case where there are 2 transmit antennas present, and they transmit the signals s_1 and s_2. When STTD is used, these two signals are simultaneously transmitted from the antennas 1 and 2 respectively in the given time instant t. During the next time instant $(t + T)$, where T is the symbol period and is proportional to the coherence time of the wireless channel, the symbol $(-s_2^*)$ is transmitted from antenna 1 and s_1^* is transmitted from antenna 2. (s^*) represents the complex conjugate of the symbol s. The receiver receives the transmitted symbols along with the channel impulse response. The received symbol can be represented as

$$r_1 = h_1 s_1 + h_2 s_2 + n_1, \tag{4.5}$$

$$r_2 = -h_1 s_2^* + h_2 s_1^* + n_2. \tag{4.6}$$

The combiner at the MS, using the channel impulse response, reconstructs the received signal resulting in the combined signals

$$s_{1c} = h_1^* r_1 + h_2 r_2^*, \tag{4.7}$$

$$s_{2c} = h_2^* r_1 - h_1 r_2^*. \tag{4.8}$$

The combined symbol is sent to a maximum likelihood detector to estimate the transmitted signal. Based on this analysis, it can be seen that the receiver does not need to send any feedback to the transmitter about the channel conditions. Higher order STBC codes are also possible, but the complexity increases linearly with the increase in the number of antennas. However, open-loop transmit-diversity method has been standardized in 3GPP for its use in both, UMTS and LTE.

It can be noted that, as expected, transmission would be more efficient if the channel information is known beforehand at the transmitter. Closed-loop

transmit-diversity schemes are used for this purpose.

4.3 Closed-Loop Transmit-Diversity

The structure of a transmitter which supports closed-loop transmit-diversity can be appreciated in Fig. 4.1. In closed-loop techniques, the MS sends the feedback to the transmitter about the channel characteristics. The feedback is considered explicit if the MS informs about the channel gain and the noise-plus-interference power without assuming any receiver or transmitter processing. The feedback can include the channel matrix, transmit covariance matrix (R_i), or the eigen values of these matrices [8]. An alternate feedback technique is implicit feedback. In this feedback method, assumption is made about the transmitter or receiver processing, and the statistical information is sent as *channel quality indicator* (CQI), *precoding matrix indicator* (PMI) or *rank indicator* (RI) matrices. The feedback is used to calculate the antenna specific transmit weights.

These antenna specific weights are chosen such that, when applied with the succeeding transmitted symbols, the MS receives the maximum SINR. Assuming that there are M transmit antennas and that there is no interference between the transmitted signals, the received signal at the MS can be written as an extension of (4.1) as follows:

$$r = (h \cdot w)s + n, \tag{4.9}$$

where s is the transmitted symbol, h represents the vector with channel gains, n is the additive white gaussian noise (AWGN) with mean power $N_0 = 1$. w represents the transmit weights that are chosen by the transmitter depending on the feedback received from the MS.
The total received power at the receiver is calculated by the relation [25]

$$\mathbb{E}\{|r|^2\} = w^H h^H h w, \tag{4.10}$$

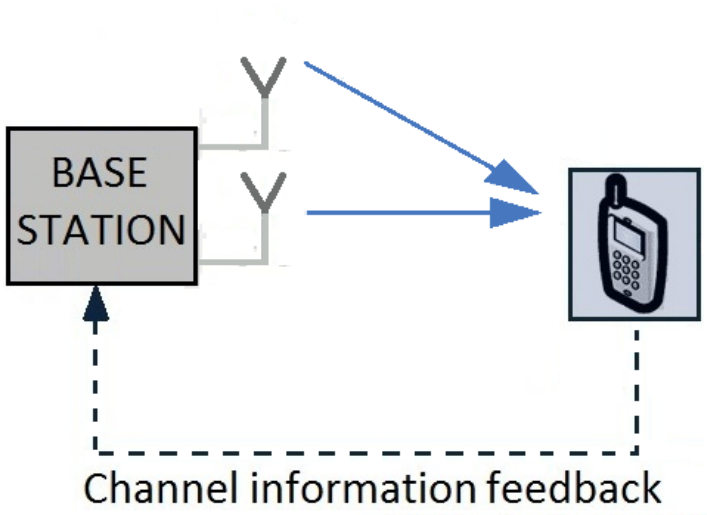

Figure 4.1: Closed loop system for two transmit antennas. The solid line indicates the signal that is transmitted to the MS, and the dotted line indicates the feedback from the MS to the BS.

w^H represents the Hermitian of the matrix w. Now, w has to be chosen such that the received power is maximized [27], i.e.,

$$\mathbb{E}\{|r|^2\}_{\max} = arg \max_{\mathrm{w}}(w^H h^H hw)\ \mathbb{E}\{|r|^2\} \tag{4.11}$$

This implies that the weights should be chosen so that the SINR at the receiver is maximum,i.e.,

$$\hat{w} = arg \max_{\mathrm{w}\in\mathcal{W}}|h \cdot w|. \tag{4.12}$$

The use of closed-loop transmit-diversity results in coherent combining gain and diversity gain [28]. The coherent combining gain is because the signals combine coherently and the interference combines non-coherently at the receiver side. An ideal coherent combining gain for a 2 antenna system is 3 dB. Diversity gain is obtained if fading processes are uncorrelated between the different antenna links. This is realized by placing the antennas sufficiently apart, typically at a distances of few wavelengths. It is also important to highlight that the propagation delays of the signals from the different transmitters to the MS is still approximately the same.

There are 3 main approaches of closed-loop transmit-diversity that have been considered in this Thesis. Transmit antenna selection (TAS), quantized cophasing, and quantized cophasing with order information. A general description of the different approaches is given in this section, and the detailed description of each of the methods is covered in the following chapters.

4.3.1 Transmit Antenna Selection

The implementation of transmit antenna selection as a diversity technique is simple. The quantization set of the weights $\mathcal{W}$ consists of vectors, which contain one element equal to unity, and all other elements are zero. This implies that at any point in time, only one antenna is active, and the other antennas are not used. Depending on the perceived channel quality strength, the transmitter applies all its power in the antenna with best gain.

Hence, we have

$$\|h\hat{w}\| = \max \|h_m\| \qquad 1 \leq m \leq M. \tag{4.13}$$

The quantization for M transmit antennas has M elements, hence $\log_2(M)$ feedback bits are needed. For example, if 4 transmit antennas are considered, the quantization set $\mathcal{W}$ will contain the vectors (1,0,0,0),(0,1,0,0,),(0,0,1,0),(0,0,0,1), and the feedback signalling demands 2 bits to represent the best antenna.

4.3.2 Quantized Cophasing

In this method, the relative phase differences between the antennas are adjusted in the transmitter using the reported feedback information. The feedback from the receiver, therefore, contains only the information about the phase difference between the received signals. One antenna among the set of M transmitting antennas is chosen as the reference antenna, and the other antennas, known as diversity antennas, have their phases adjusted according to the phase of the signal from the reference antenna. The feedback word length depends on the resolution that is needed. The weights are calculated

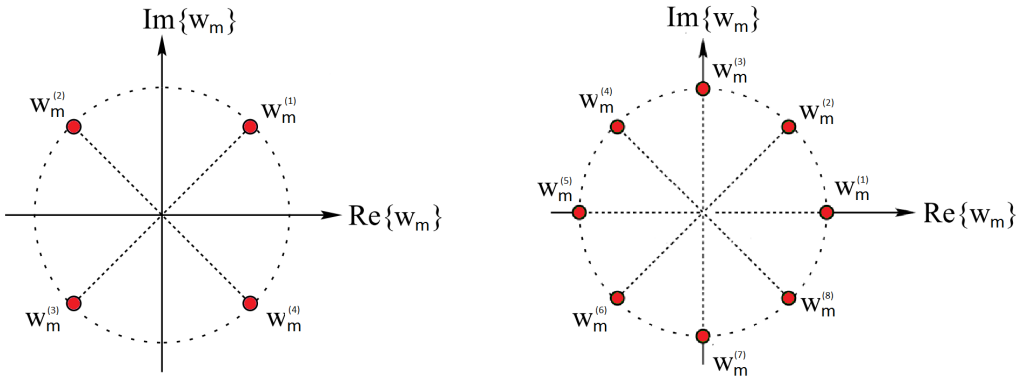

(a) 2-bit feedback word (b) 3-bit feedback word

Figure 4.2: Feedback quantization set for different quantized cophasing schemes.

according to the following relation:

$$(w_1, w_m) = \frac{1}{\sqrt{M}} \left(1, e^{j\left[\frac{2\pi(n-1)}{2^N}\right]}\right) \quad n \in \{1, 2, ..., 2^N\}, \tag{4.14}$$

so that

$$|h_1 + \hat{w}_m h_m| = \max_{w_m \in \mathrm{W_N}} |h_1 + w_m h_m| \tag{4.15}$$

takes place.

Two sample quantization sets for 2-bit and 3-bit feedback resolution is given in Figs. 4.2a and 4.2b, respectively.

This method is also referred to as closed-loop mode 1 in 3GPP standards [25]. As the number of transmitting antennas increases, there is a corresponding linear increase in the complexity of quantized cophasing. However, when the number of transmit antennas is not high, this method can be implemented in a fairly easy way.

4.3.3 Quantized Cophasing with Order Information

This method can be considered as an extension of quantized cophasing. In this method, the essence of quantized cophasing is used, along with the ad-

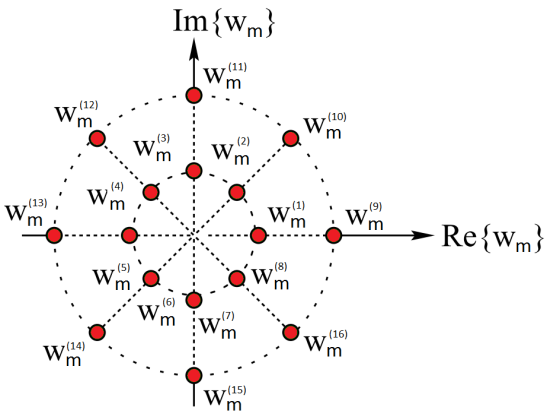

Figure 4.3: Feedback weights for Quantized Cophasing with order information. The feedback resolution for this method is 4 bits. 3 bits are required to represent the phase information, and 1 bit for the order information.

vantages of TAS. In quantized cophasing with order information, the power information is also used along with the phase information to determine the weights. The recommended amplitude weights if 2 antennas are considered is $(0.8, 0.2)$. This follows from the fact that there is an improved performance gain if more power is put on the antennas with stronger channel gains. This method is also referred to as closed-loop mode 2 in 3GPP specifications [25].

The weights for quantized cophasing with order information, when 2 transmitters are used, is shown in Fig. 4.3 [29]. It must be kept in mind that the numbers indicated in the figures are only meant to show the different possibilities in the quantization set. In real systems, the different symbols are coded using Gray codes to minimize the effect of feedback error.

The different channels can be sorted according to powers, and the amplitude weights can be applied to the different antennas. When the number of antennas is low, the order information can be quantized into weights easily. As the number of antennas increase, the quantization of amplitude weights is difficult and inaccurate. This method of transmit diversity is not considered in this Thesis.

Chapter 5

Performance Analysis and Simulations

The concepts explained in the previous chapters were used to build a simulator in order to study a cooperative multipoint transmission system. A continuous channel, based on Jakes' model is produced for the study. Analytical relations are derived to compare them with the numerical simulation results, as a simple way to validate the simulator.
In this chapter, the simulations as well as the derivations are explained in detail. The obtained results and the comparison of the analysis of the different diversity techniques are also discussed.

5.1 Impact of Delay on BER of Transmit Diversity Techniques

The bit error rate and the probability of error, P_e, were presented in (3.15). For a given SNR value, $\bar{\gamma}$, P_e can be written as

$$P_e(\bar{\gamma}) = \int_0^\infty p(\gamma) \cdot e(\gamma) d\gamma. \tag{5.1}$$

The probability of error is known in the case of BPSK, and is given by (4.3). In the case of more complex modulation techniques, the probabilities of error

were calculated. In this section, the study done in [30] is followed, to arrive at the relation for the value of P_e. These analytical values are then compared with the simulations, in order to confirm the validity of the simulator.

For a transmission using transmit diversity, $e(\bar{\gamma})$ value is given in [31] as

$$e(\bar{\gamma}) = \int_0^\infty (\bar{\gamma} \cdot z(\gamma, \phi)) e^{-|\gamma|} d\gamma. \tag{5.2}$$

Equating (5.1) in (5.2), and simplifying as in [31] and [30], the P_e for a 2 antenna case of quantized cophasing and quantized cophasing with order information can be approximated as

$$P_e(\bar{\gamma}) = \frac{1}{4}\left(1 - \sqrt{\left(\frac{\bar{\gamma}/2}{C_{2,N} + \bar{\gamma}/2}\right)}\right)^2 \cdot \left(2 + \sqrt{\frac{\bar{\gamma}/2}{C_{2,N} + \bar{\gamma}/2}}\right), \tag{5.3}$$

where $C_{2,N}$ is a term that is related the complex generic term term $A_{M,N}$, defined by

$$A_{M,N} = \left\{ \frac{(M-1)!}{M^M} \int_{\Omega_\phi} \int_{\mathbb{R}^{M-1}} \frac{f(\phi) dr d\phi}{z(r,\phi)^M} \right\}^{\frac{1}{M}}. \tag{5.4}$$

Figure 5.1 shows the BER curves as a function of SNR when 2 transmit antennas are used. It is assumed that the speed of the receiver is 36 km/h. Similar to the work done in [31], 10×10^6 samples were used to obtain these plots.

Next, a delay is introduced, and its effect is studied. Figure 5.2 gives the performances of the different methods when feedback delay is present. Figure 5.2a gives the BER of the system when there is a delay of 1 slot. Comparing it with the Fig. 5.1, we can see that the bit error rate has worsened with the addition of delay. The trend continues with the addition of more delay, as seen from the Figs. 5.2b, 5.2c, and 5.2d. The performance of the system, therefore, impairs with the increase in delay, and tends to perform like a single antenna system. At very high delay, the diversity gain is lost, and the system performs like a single antenna system.

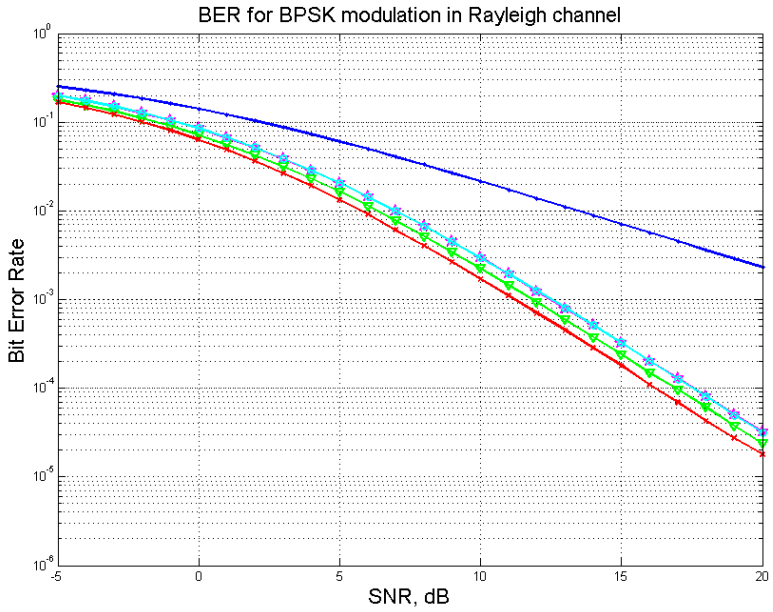

Figure 5.1: BER curves as a function of SNR for the different transmit diversity techniques. The BER of transmit antenna selection (magenta, $\star$) and quantized cophasing with 1 bit feedback (cyan, $\circ$) overlap to indicated same performance. Bit error rate of quantized cophasing with 2 bit feedback information (green, $\bigtriangledown$) and quantized cophasing with order information (amplitude weights of $(0.8, 0.2)$) (red, $\times$) are also shown. The single antenna system (blue, $\bullet$) is considered as baseline and as an upper bound for performance.

We can also see that finding analytical relations for the BER is complex in the case of transmit diversity techniques, and hence, SNR gain, introduced in section 3.6.2, will be used as a performance measure. The performance of the transmit diversity techniques, TAS and quantized cophasing, and a combination of these two methods to form a hierarchical signalling scheme is studied in the next sections.

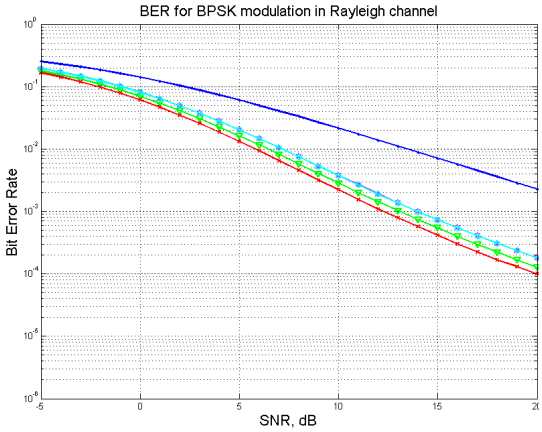

(a) delay = 1 slot

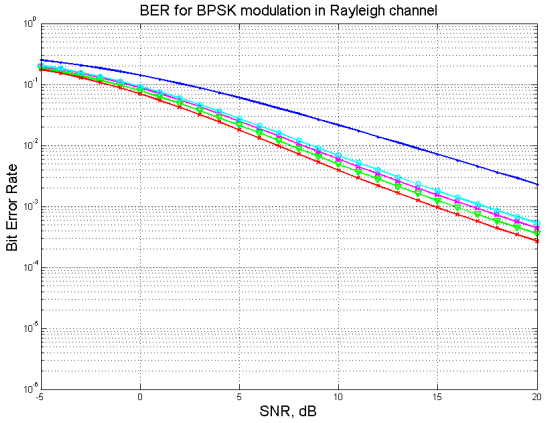

(b) delay = 2 slots

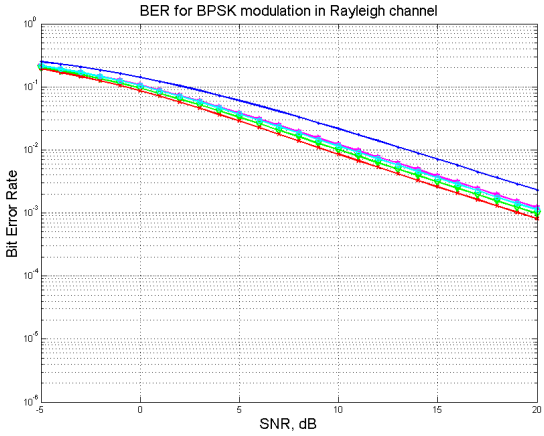

(c) delay = 3 slots

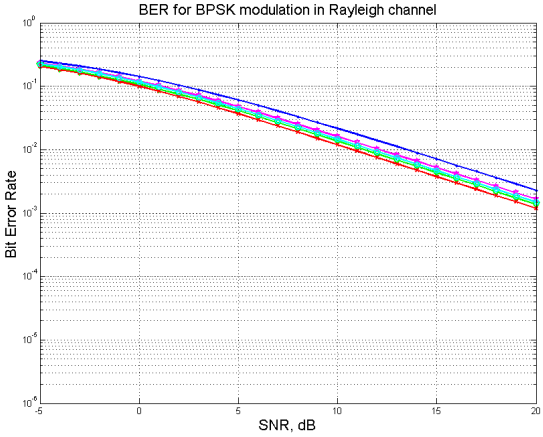

(d) delay = 4 slots

Figure 5.2: Effect of delay on the BER of transmit diversity techniques. The BER of transmit antenna selection (magenta, $\star$) and quantized cophasing with 1 bit feedback (cyan, $\circ$) overlap to indicated similar performance. Bit error rate of quantized cophasing with 2 bit feedback information (green, $\bigtriangledown$) and quantized cophasing with order information (amplitude weights of $(0.8, 0.2)$) (red, $\times$) are also shown. The single antenna system (blue, $\bullet$) is considered as baseline and as an upper bound performance.

5.2 Signal-to-Noise power Ratio Gain of Transmit Antenna Selection

We now derive the expression for the SNR Gain of TAS to study its performance.

5.2.1 Transmit Antenna Selection with no Feedback Delay

In a TAS system, the antenna with the best perceived channel quality (i.e., with the highest value of SNR) is selected, and all the power is transmitted through it. We now assume that the signals from each transmitter are uncorrelated, and have Rayleigh distributed power with mean P_0. The PDF of the signal envelope is therefore given by

$$p(r_m) = \frac{r_m}{P_0} e^{-\frac{{r_m}^2}{2P_0}}, \quad r_m \geq 0, \tag{5.5}$$

where r_m represents the envelope of the signal from the m^{th} transmitter. The expected value of power per branch is ${r_m}^2/2$. Assuming the noise per branch to be equal to N_{br}, we now have

$$\gamma_m = \frac{\text{signal power per branch}}{\text{mean noise power per branch}} = \frac{{r_m}^2}{2N_{br}}. \tag{5.6}$$

The total expected value of SNR of the system is

$$\Gamma = \mathbb{E}\langle\gamma_{\text{tot}}\rangle = \frac{P_0}{N_{br}}. \tag{5.7}$$

The PDF of SNR is given by

$$p(\gamma_m) = \frac{1}{\Gamma} e^{-\frac{\gamma_m}{\Gamma}}. \tag{5.8}$$

The Cumulative Distribution Function (CDF) of SNR in one branch being less

than or equal to some specific value γ is

$$P[\gamma_m \leq \gamma] = \int_0^{\gamma} P(\gamma_m) d\gamma_m = 1 - e^{\frac{-\gamma}{\Gamma}}. \tag{5.9}$$

This relation can be extended when the SNR of all the M branches is less than or equal to γ, and is given by

$$P[\gamma_1 \cdots \gamma_M \leq \gamma] = (1 - e^{\frac{-\gamma}{\Gamma}})^M = P_M(\gamma). \tag{5.10}$$

We know from [21] that the SNR gain can be obtained from the PDF by using the relation

$$\mathbb{E}\langle\gamma\rangle = \int_0^{\infty} \gamma p_M(\gamma) d\gamma, \tag{5.11}$$

and PDF is the differential of CDF, given by

$$p_M(\gamma) = \frac{d}{d\gamma} P_M(\gamma) = \frac{M}{\Gamma}(1 - e^{-\frac{\gamma}{\Gamma}})(e^{-\frac{\gamma}{\Gamma}}). \tag{5.12}$$

Therefore, substituting (5.12) in (5.11), the SNR gain is obtained to be

$$\mathbb{E}\langle\gamma\rangle = \Gamma \sum_{m=1}^{M} \frac{1}{m}. \tag{5.13}$$

The derivation from [21] was followed to arrive at this relation, and the value of SNR gain obtained is valid only when there is no feedback delay.

Next, we derive a closed form expression for the SNR gain of TAS in the presence of feedback delay.

5.2.2 Transmit Antenna Selection with Feedback Delay

In the presence of delay D, the PDF of the SNR given in (5.12) will change, and can be written as given in [7], i.e.,

$$p(\gamma_D) = \sum_{m=0}^{M-1} \frac{M/\Gamma}{[m(1-\rho)+1]} \cdot (-1)^m \binom{M-1}{m} e^{\left(-\frac{\alpha}{\gamma_D}\right)}, \tag{5.14}$$

where $\alpha = \frac{m+1}{\gamma_0[m(1-\rho)+1]}$ and $\rho = J_0^2(2\pi f_d T_s D)$. $J_0(\cdot)$ is the 0-th order Bessel function, T_s is the time duration of one slot, and f_d is the doppler frequency. $\binom{M-1}{m}$ represents the binomial coefficient indexed by (M-1) and m.

Again, substituting (5.14) in (5.11) we can get the expression for the SNR gain for TAS in the case of delay, i.e.,

$$\mathbb{E}\langle\gamma_D\rangle = \int_0^\infty \gamma_D \sum_{m=0}^{M-1} \frac{M/\Gamma}{[m(1-\rho)+1]} \cdot (-1)^m \binom{M-1}{m} e^{\left(-\frac{\alpha}{\gamma_D}\right)} d\gamma_D. \quad (5.15)$$

The general equation for all values of M can be solved to obtain a closed-form expression, but the solution is complex and is omitted in this study. A solution is presented for the case where M = 2 transmit antennas, where the mean SNR, Γ, is unitary, i.e.,

$$\begin{aligned} \mathbb{E}\langle\gamma_D\rangle &= \int_0^\infty \gamma_D \sum_{m=0}^{1} \frac{2}{[m(1-\rho)+1]} \cdot (-1)^m \binom{1}{m} e^{\left(-\frac{\alpha}{\gamma_D}\right)} d\gamma_D \quad (5.16) \\ &= \int_0^\infty \gamma_D \left[2e^{-\gamma_D} - \frac{2}{2-\rho} e^{-\frac{2\gamma_D}{2-\rho}}\right] d\gamma_D. \quad (5.17) \end{aligned}$$

Solving the integral, we get

$$\mathbb{E}\langle\gamma_D\rangle = 1 + \frac{\rho}{2}. \quad (5.18)$$

Using this relation, the analytical and simulation results were compared. The resulting plots are shown in Fig. 5.3

From these figures, it can be seen that the gain reduces when the speed of the terminal increases. Gain reduction becomes more evident in the case of more delay. For example, when there is a 3 slot delay, the advantage of using TAS is lost at a speed of about 80 km/h. It can also be observed that the use of TAS does not provide a good SNR gain even in case of low delays. Hence, better methods have to be used. The performance of other methods are now studied, to check if they can perform better in similar environments.

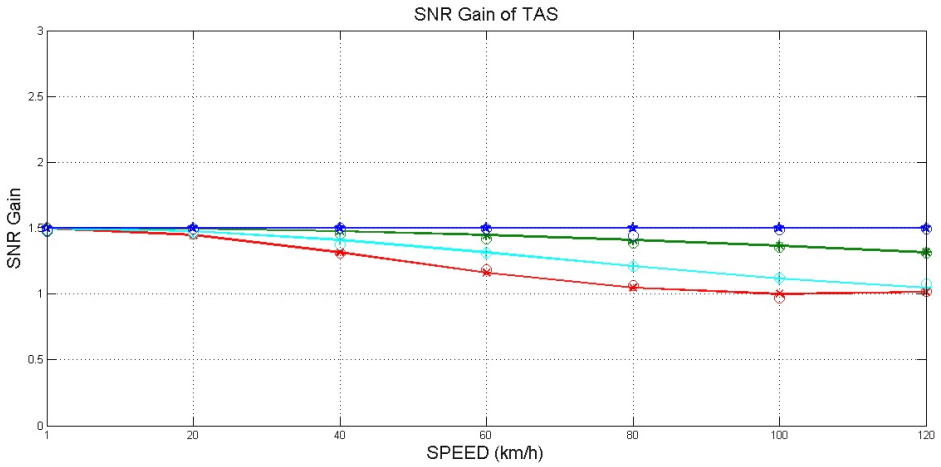

Figure 5.3: SNR gain (linear) of TAS with respect to receiver velocity. The analytical values of SNR gain for a delay of 0 (blue, $\star$), 1 slot (green, $*$), 2 slots (cyan, $+$), 3 slots (red, $\times$) are compared with the simulated values ($\circ$).

5.3 Signal-to-Noise power Ratio Gain of Quantized Cophasing

In this section, the SNR gain of quantized cophasing when there is no delay is derived according to [23]. The SNR gain with feedback delay is presented in the power balanced case, when the mean powers from all the transmitters are equal to the unitary value.

5.3.1 Quantized Cophasing with no Feedback Delay

When there is no feedback delay, the expression for the SNR gain is straightforward, and can be obtained, as shown in [23]. The phases of the different coefficients of the channel will be uniformly distributed in the interval $(-\pi, \pi)$, and the channel coefficients can be written as $h_m = \alpha_m e^{j\phi_m}$, where $m = 1, 2, \cdots, M$. After quantized cophasing is used and the transmit beamforming weights are applied, the phases $\Psi = \phi_m + \arg(w_m)$ are now uniformly distributed in the interval $\left(-\frac{\pi}{2^N}, \frac{\pi}{2^N}\right)$, where N represents the number of feedback bits.

The SNR gain given by (3.16) can be written as

$$\mathbb{E}\langle\gamma\rangle = \frac{\mathbb{E}\langle|wh|^2\rangle}{\mathbb{E}\langle\alpha_M^2\rangle}, \tag{5.19}$$

where $\alpha_M = |h|$. The value of $\langle|wh|^2\rangle$ now needs to be derived. By using a closed-loop signalling system equation as described in section 4.3, we have from [23] that

$$|wh|^2 = \sum_{m=1}^{M} |w_m|^2\alpha_m^2 + 2\sum_{m=2}^{M}\sum_{k=1}^{m-1} |w_m|\ \alpha_m\ |w_k|\ \alpha_k \cos(\Psi_m - \Psi_k), \tag{5.20}$$

where $\mathbb{E}\langle\cos(\Psi_m - \Psi_k)\rangle$ can be simplified for $m \neq k$, and can be re-written as

$$\mathbb{E}\langle\cos(\Psi_m - \Psi_k)\rangle = \begin{cases} c_N & \text{when m = 1 or k = 1,} \\ {c_N}^2 & \text{otherwise,} \end{cases}$$

where

$$c_N = \left(\frac{2^N}{\pi}\right)\sin\left(\frac{\pi}{2^N}\right). \tag{5.21}$$

Setting $|w_m| = \frac{1}{\sqrt{M}}$, we now have from (5.20) that

$$\mathbb{E}\langle|wh|^2\rangle = \mathbb{E}\langle\alpha_M^2\rangle + (M-1)\left(1 + \frac{M-2}{2}c_N\right)\frac{2c_N}{M}\cdot\mathbb{E}\langle\alpha_m\alpha_k\rangle. \tag{5.22}$$

Substituting 5.22 in 5.19, we have

$$\mathbb{E}\langle\gamma\rangle = 1 + (M-1)\left(1 + \frac{M-2}{2}c_N\right)\frac{2c_N}{M}\frac{\mathbb{E}\langle\alpha_m\alpha_k\rangle}{\mathbb{E}\langle{\alpha_m}^2\rangle}. \tag{5.23}$$

In case of a Rayleigh fading channel model, we have from [23],

$$\frac{\mathbb{E}\langle\alpha_m\alpha_k\rangle}{\mathbb{E}\langle{\alpha_m}^2\rangle} = \sqrt{\pi}. \tag{5.24}$$

Therefore, we have the SNR gain of quantized cophasing, when there is no

delay as

$$\mathbb{E}\langle\gamma\rangle = 1 + (M-1)\left(1 + \frac{M-2}{2}c_N\right)\frac{2c_N}{M}\sqrt{\pi}. \tag{5.25}$$

5.3.2 Quantized Cophasing with Feedback Delay

In the presence of feedback delay, the performance of a quantized cophasing transmission scheme deteriorates. In this section, the analysis is done with a finite feedback delay based on [6].

Equation (5.20) can be rewritten, when there is one reference antenna, and all the other antennas are cophased according to the reference antenna, such that there are 3 distinct terms in the equation. The first term is related to the individual transmitters, the second term is the product of the channel response of the reference antenna and the diversity antennas (after adjusting the phases), and all the remaining factors form the third term, i.e.,

$$\begin{aligned}|wh|^2 = \sum_{m=1}^{M} |w_m|^2\alpha_m^2 + 2\sum_{k=2}^{M} |w_1|\ |w_k|\ \alpha_1\ \alpha_k \cos(\Psi_1 - \Psi_k) \\ + 2\sum_{m=3}^{M}\sum_{k=2}^{m-1} |w_m|\ \alpha_m\ |w_k|\ \alpha_k \cos(\Psi_m - \Psi_k).\end{aligned} \tag{5.26}$$

The expected value of $|wh|^2$ needs to be calculated now, and similar to the expression for the SNR gain when there is no delay, the first term reduces to unity.

According to [6], the second term can be reduced into

$$2\sum_{k=2}^{M} |w_1|\alpha_1|w_k|\alpha_k \cos(\Psi_1 - \Psi_k) = \frac{M-1}{2M}\pi c_N \rho^2. \tag{5.27}$$

Finally, the third term can be simplified to

$$2\sum_{m=3}^{M}\sum_{k=2}^{m-1} |w_m|\ |w_k|\ \alpha_m\ \alpha_k \cos(\Psi_m - \Psi_k) = \frac{(M-1)(M-2)}{4M}\pi c_N^2 \rho^2, \tag{5.28}$$

where $\rho = J_0^2(2\pi f_d T_s D)$ and c_N is the factor defined in (5.21)

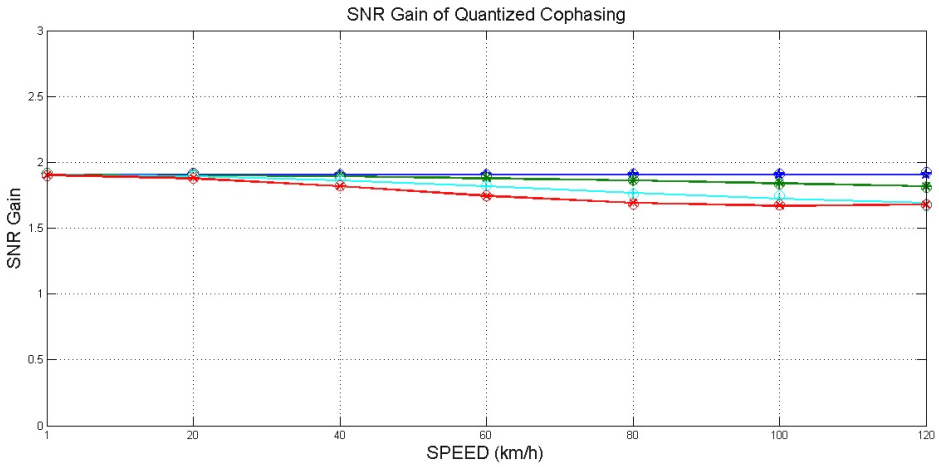

Figure 5.4: SNR gain (linear) of quantized cophasing with respect to receiver velocity. The analytical values of SNR gain for a delay of 0 (blue, $\star$), 1 slot (green, $*$), 2 slots (cyan, $+$), 3 slots (red, $\times$) are compared with the simulated values ($\circ$).

Then, the expression for the SNR gain becomes

$$\mathbb{E}\langle\gamma_D\rangle = 1 + \frac{M-1}{2M}\pi c_N \rho^2 \left(1 + \frac{M-2}{2} c_N\right). \tag{5.29}$$

When there are 2 transmit antennas, the value of $\mathbb{E}\langle\gamma_D\rangle$ reduces to

$$\mathbb{E}\langle\gamma_D\rangle = 1 + \frac{\pi c_N \rho^2}{4}. \tag{5.30}$$

Using the above relation, the SNR gains of quantized cophasing was generated both, analytically and through the aid of simulations, and they are shown in Fig. 5.4.

The figure 5.4 plots the SNR gain of a quantized cophasing system against the receiver velocity. Comparing this system with a TAS system in Fig. 5.3, it can be seen that the performance of quantized cophasing is notably improved.
It is then necessary to study the performance of quantized cophasing in different environments, so that an optimum transmit diversity method could be devised.

5.4 Signal-to-Noise power Ratio Gain of Quantized Cophasing in Power Imbalance Case

Transmit-diversity methods are generally applied to cell edge users, where channel amplitudes are assumed to be with perfect power balance. However, it is possible that the receive powers are unequal from the different transmitters due to the environment or the profile of the user. The power imbalance may also have an effect on the performance of the system, and this demands the need to study the effect of delay for quantized cophasing in power imbalance situations.

The derivation of the closed form general expression for SNR gain of a quantized cophasing system forms the major part of this Thesis. The derivation follows closely the expression derived in section 5.3.2, but it now considers that the received power is different from the different antennas. Derivation in this section is based on [6], and can be considered as an extension to it. A simple illustration that shows the power imbalance condition can be appreciated in Fig. 5.5. As seen, one reason for the power imbalance situation would be due to unequal distances from the transmitters, in this precise case, (d1 $<$ d2), which naturally causes the received power levels to be different, i.e., ($\mathbb{E}\{|r_1|^2\} > \mathbb{E}\{|r_2|^2\}$).

The difference in the powers in dB indicates the value of imbalance. Table 5.1 gives the different power values of the transmitters corresponding to the different power imbalance situations.

In section 5.3.2, we have considered that the mean powers from the different transmitters are all equal to unitary value. In the case of imbalance, we now consider that the mean powers are not equal to unity, but some value Υ. The channel gain vector, in the case of channel imbalance case is now represented

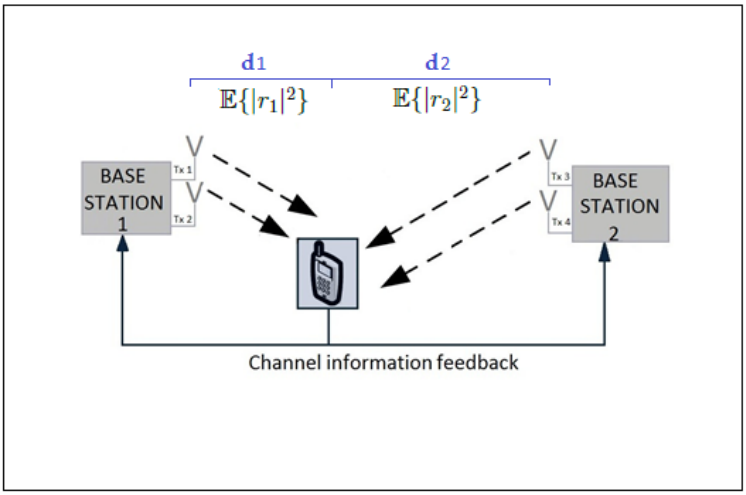

Figure 5.5: Example of power imbalance situation. The illustration shows the receiver to be at different distances (d1, d2) from the base station, resulting in different receive power values ($\mathbb{E}\{|r_1|^2\}$,$\mathbb{E}\{|r_2|^2\}$)

Table 5.1: Power imbalance and corresponding power values. Normalization was carried out such that the total received power is always equal in all cases.

Power Imbalance	Mean power $\mathbb{E}\{|r_1|^2\}$	Mean power $\mathbb{E}\{|r_2|^2\}$
5 dB	1.2801	0.7198
10 dB	1.5194	0.4805
15 dB	1.6980	0.3019
20 dB	1.8181	0.1818

as $\widetilde{h}$. Consequently,

$$\mathbb{E}|\widetilde{h}_m|^2 = \Upsilon_m, \quad m \in \{1, 2, \cdots, M\}, \tag{5.31}$$

and

$$\Upsilon_1 + \Upsilon_2 + \cdots + \Upsilon_M = M. \tag{5.32}$$

Using the above relations in (5.31) and (5.32), the SNR gain of the system can

now be derived by rewriting (5.20) as

$$|w\widetilde{h}|^2 = \sum_{m=1}^{M}\sum_{k=1}^{M} w_m \widetilde{h}_m {w_k}^* \widetilde{h}_k^*. \tag{5.33}$$

The expansion of the above summation results in an equation consisting of 3 distinct terms, like in the case of equation (5.26), and can be written as

$$|w\widetilde{h}|^2 = \sum_{m=1}^{M} |w_m|^2|\widetilde{h}_m|^2 + 2\sum_{k=2}^{M} |w_1\widetilde{h}_1 {w_k}^*\widetilde{h}_k^*| + 2\sum_{m=3}^{M}\sum_{k=2}^{m-1} |w_m\widetilde{h}_m {w_k}^*\widetilde{h}_k^*|. \tag{5.34}$$

The SNR gain is the expectation of the previous expression, i.e.,

$$\mathbb{E}\langle\gamma_D\rangle = \mathbb{E}\langle|w\widetilde{h}|^2\rangle \tag{5.35}$$

The expectation of each term of (5.34) can be found individually, and then summed to get the value of $\mathbb{E}\langle\gamma_D\rangle$. Therefore, the first term in the summation can be simplified as

$$\mathbb{E}\left\langle \sum_{m=1}^{M} |w_m|^2|\widetilde{h}_m|^2 \right\rangle = 1, \tag{5.36}$$

using (5.31) and (5.32).
In addition, the samples of $|\widetilde{h}_m|$ follow Rayleigh distribution, and $|w_m| = 1/\sqrt{M}$. Furthermore, $\widetilde{h}$ can be simplified as $h\sqrt{\Upsilon}$, and $\mathbb{E}|h|^2 = 1$. Using this, and with simplification, we get

$$\mathbb{E}\left\langle \sum_{k=2}^{M} |w_1\widetilde{h}_1 {w_k}^*\widetilde{h}_k^*| \right\rangle = \sum_{k=2}^{M} \sqrt{\Upsilon_1}\cdot\sqrt{\Upsilon_k}\frac{\pi}{4M}\mathbb{E}\langle e^{j(\phi_1(t)-\phi_k(t)-\psi_k)}\rangle, \tag{5.37}$$

where $\phi(t)$ is the phase of h, and it is assumed that $w_k = 1/\sqrt{M}e^{j\psi_k}$. We first simplify $e^{j(\phi_1(t)-\phi_k(t)-\psi_k)}$ in (5.37) by adding and subtracting $\phi_1(t-\tau)-\phi_k(t-\tau)$ from the powers. Here, $(t-\tau)$ is the instant at which weight is chosen. The variable τ represents that delay, and it is equal to $T_s\ D$.

Therefore, we can write

$$\begin{aligned}&\phi_1(t) - \phi_k(t) - \psi_k - \big(\phi_1(t-\tau) - \phi_k(t-\tau)\big) + \big(\phi_1(t-\tau) - \phi_k(t-\tau)\big)\\ &= \big(\phi_1(t) - \phi_1(t-\tau)\big) - \big(\phi_k(t) - \phi_k(t-\tau)\big) + (\phi_1(t-\tau) - \phi_k(t-\tau) - \psi_k)\\ &= \Delta\phi_1(t) - \Delta\phi_k(t) + \varphi_k, \quad (5.38)\end{aligned}$$

where

$$\varphi_k = (\phi_1(t-\tau) - \phi_k(t-\tau) - \psi_k). \quad (5.39)$$

The variable φ_k in uniformly distributed in the the range $\big(-\frac{\pi}{2^N}, \frac{\pi}{2^N}\big)$ which results in

$$\mathbb{E}\langle \sin\varphi_k \rangle = 0, \quad \mathbb{E}\langle \cos\varphi_k \rangle = c_N. \quad (5.40)$$

Now, writing the exponential terms of (5.37) using (5.38) in terms of cosine and sine functions, we have,

$$\begin{aligned}e^{j(\Delta\phi_1(t) - \Delta\phi_k(t) - \varphi_k)} &= e^{j(\Delta\phi_1(t) - \Delta\phi_k(t))} \cdot e^{-j(\varphi_k)} && (5.41)\\ &= e^{j(\Delta\phi_1(t) - \Delta\phi_k(t))} \cdot (\cos\varphi_k + i\sin\varphi_k) && (5.42)\\ &= e^{j(\Delta\phi_1(t) - \Delta\phi_k(t))} \cdot c_N. && (5.43)\end{aligned}$$

As the different channels are considered to be uncorrelated, the random variables $\Delta\phi_1(t)$ and $\Delta\phi_k(t)$ are independent and identically distributed (i.i.d.). The above expression could further be simplified and its expectation can be written as

$$\mathbb{E}\left\langle c_N \; e^{j(\Delta\phi_1(t) - \Delta\phi_k(t))} \right\rangle = c_N \; \mathbb{E}\langle \cos(\Delta\phi(t)) \rangle^2. \quad (5.44)$$

When the receiver is moving at a velocity v, it can be considered that the system with delay simplifies as a system with spatially separated antennas, with distance $d = v\tau$ between them. So, $\phi(t) = \phi(t-\tau) + \frac{2\pi}{\lambda} d\cos\psi$, where ψ

is uniformly distributed on $(-\pi, \pi)$, i.e.,

$$c_N \cdot \mathbb{E}\langle \cos(\Delta\phi(t)) \rangle^2 = c_N \left[\frac{1}{2\pi} \int_{-\pi}^{\pi} \cos\left(\frac{2\pi}{\lambda} v\tau \cos\psi \right) d\psi \right]^2 \quad (5.45)$$

$$= c_N \left[J_0 \left(\frac{2\pi}{\lambda} v\tau \right) \right]^2 \quad (5.46)$$

$$= c_N \left[J_0 \left(2\pi f_d T_s D \right) \right]^2. \quad (5.47)$$

Substituting (5.47) in (5.37), we have

$$\mathbb{E}\left\langle 2 \sum_{k=2}^{M} |w_1 \widetilde{h}_1 {w_k}^* \widetilde{h}_k^*| \right\rangle = \frac{\pi}{2M} c_N J_0^2 \left(2\pi f_d T_s D \right) \sum_{k=2}^{M} \sqrt{\Upsilon_1 \, \Upsilon_k}. \quad (5.48)$$

The third term of (5.34) can be solved similar to the solution above. The term equivalent to (5.38) will have 2 terms corresponding to φ_k and φ_m, and the resulting expectation value $\mathbb{E}\langle \cos(\varphi_m - \varphi_k) \rangle$ would be equal to c_N^2. Therefore,

$$\mathbb{E}\left\langle 2 \sum_{m=3}^{M} \sum_{k=2}^{m-1} |w_m \widetilde{h}_m {w_k}^* \widetilde{h}_k^*| \right\rangle = \frac{\pi}{2M} c_N^2 J_0^2 \left(2\pi f_d T_s D \right) \sum_{m=3}^{M} \sum_{k=2}^{m-1} \sqrt{\Upsilon_m \, \Upsilon_k}. \quad (5.49)$$

combining (5.36), (5.48) and (5.49) in (5.35), we get

$$\mathbb{E}\langle \gamma_D \rangle = 1 + \frac{\pi}{2M} c_N J_0^2 \left(2\pi f_d T_s D \right) \left[\sum_{k=2}^{M} \sqrt{\Upsilon_1 \, \Upsilon_k} + c_N \sum_{m=3}^{M} \sum_{k=2}^{m-1} \sqrt{\Upsilon_m \, \Upsilon_k} \right]. \quad (5.50)$$

This is the general equation for the SNR gain for quantized cophasing. The relation can be used in the case of power imbalance, and in the presence of delay. The performance of quantized cophasing can be studied using this equation.

The number of transmit antennas and feedback resolution bits can be varied and the performance of the system can be studied in the case of different power imbalance conditions to choose the most advantageous transmission.

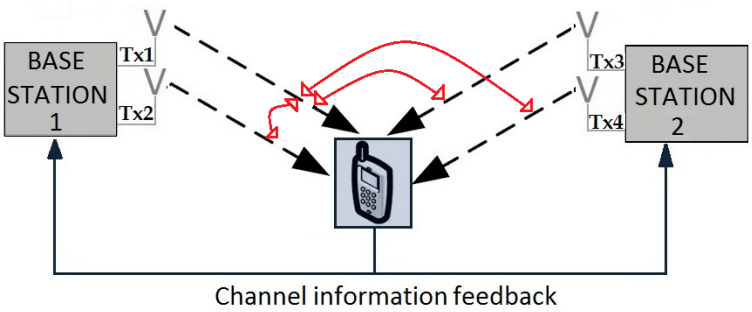

Figure 5.6: Quantized cophasing system considered for analysis. Two base stations equipped with two transmit antennas are assumed. The downlink transmission (black dashed lines) and the uplink feedback transmission (black solid line) is shown. The red lines indicate the cophasing procedure with respect to reference antenna Tx1.

5.5 Performance of Quantized Cophasing

Using the relation derived in (5.50), the performance of a quantized cophasing system can now be studied in varying conditions. In all the cases, a system as shown in Fig. 5.6 is considered, which consists of 2 BSs equipped with 2 transmit antennas each. The signals from all the antennas are cophased according to one reference antenna. It is assumed that the delays are equal for all the antennas.

5.5.1 Effect of Power Imbalance

In this section, we first study the effect of power imbalance on the SNR Gain of the system. The different channel power imbalance values that are used are 5 dB, 10 dB and 15 dB, and the corresponding values of SNR gains were obtained by both, analytical derivation and numerical simulations.

Figure 5.7 shows the SNR gain of a system described above at different channel power imbalance situations, when there are 4 transmit antennas and 2 feedback bits. As seen in the figure, as the power imbalance increases, the SNR gain gradually reduces. When the channel power imbalance is very high, it means that the receiver is very close to only one of transmitters, therefore,

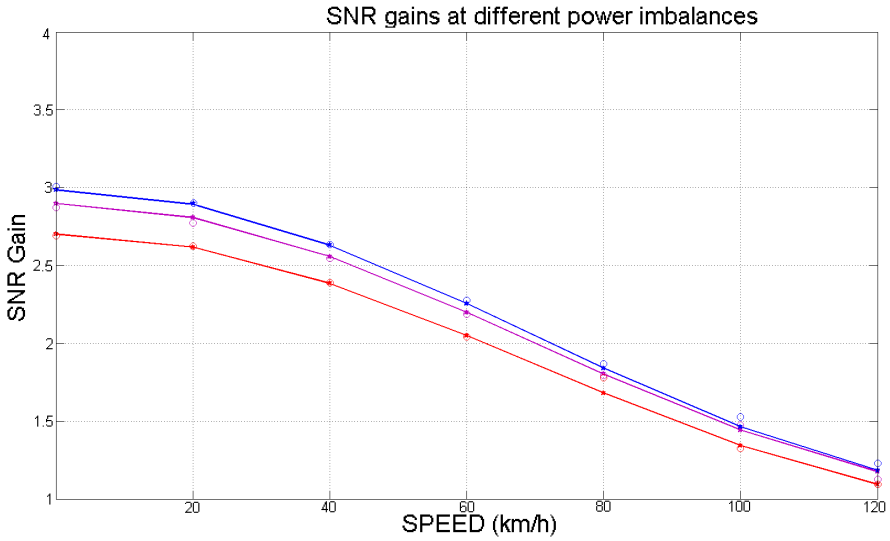

Figure 5.7: SNR gain vs receiver velocity for quantized cophasing in different power imbalance conditions. The simulation (∘) and analytical values (solid line, ⋆) are as shown for 5 dB (blue), 10 dB (magenta), 15 dB (red) channel imbalance condition.

the received powers from the other transmitters are very low. The diversity is hence lost, and the system performance follows the performance of a traditional 2 antenna system without multicell cooperation.

5.5.2 Effect of Feedback Resolution

After analyzing the effect of power imbalance, the effect of different feedback resolutions on the system with delays was studied. The total number of transmitters was set to 4, and the number of feedback bits per transmitter were chosen to be 1, 2 and 3, respectively. The figures showing the quantization of the feedback resolution can be appreciated in Fig. 4.2.

The SNR gains at different receiver velocities for the system with different feedback resolutions were analytically derived and compared with the simulations. Figure 5.8 shows the effect of feedback resolution on the performance of the system.

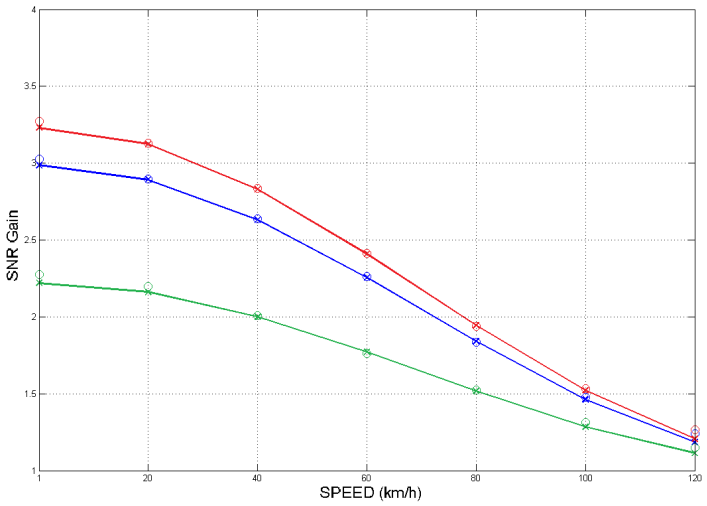

(a) SNR gain vs receiver velocity. Delay = 2 slots

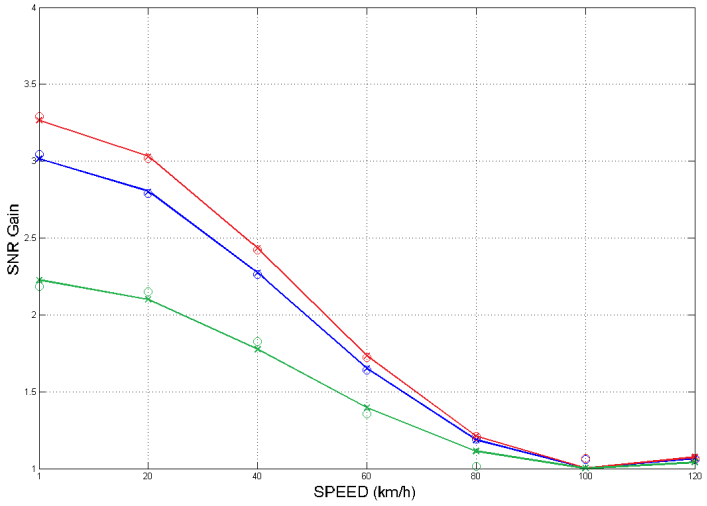

(b) SNR gain vs receiver velocity. Delay = 3 slots

Figure 5.8: SNR gain with varying feedback resolutions for quantized cophasing. The simulated values (∘) and the analytical values (solid line, ×) are shown for feedback resolution of 1-bit (green), 2-bits (blue) and 3-bits (red) for different values of delay.

It is assumed that the feedback channel has constant capacity, and that the increase in feedback bits does not imply an increase in feedback delay. Although

this assumption causes an overhead in the uplink systems, several proposals like wavelet transform, where high resolution feedback is sent in good channel conditions [32], and adaptive feedback schemes mentioned in [33] can be used to mitigate the problem of feedback overhead.

From Fig. 5.8, it can be concluded that high number of feedback bits improve the SNR gain only at low receiver velocities. As the velocity increases, the performance of all the systems with different feedback resolutions tend to be similar and there is no notable gain observed.

5.5.3 Effect of Number of Transmitters

After the analysis of the feedback resolution, the effect on the SNR gain in the case of different number of transmit antennas is studied. In this case, the number of transmit antennas is varied such that, at each time, the number of transmitters is 2, 3 and 4, and the feedback resolution is fixed to 2 bits. The performance is studied in the case of power balanced case.

The figure 5.9 shows the performance of the system when the number of transmitters is varied. From these figures, it can be seen that a high number of transmitters result in a high gain only in case of low speeds, and as the speed of the terminal increases, the performance of the system using high number of transmitters decreases.

5.6 Summary

As a summary to the analysis of quantized cophasing, Fig. 5.10 shows an example where the transition points are defined in a system using quantized cophasing.Based on the obtained results, and from the graphs in Figs. 5.8 and 5.9, the approximate coordinated transmission area can be defined based on the velocity and the power imbalance situations.

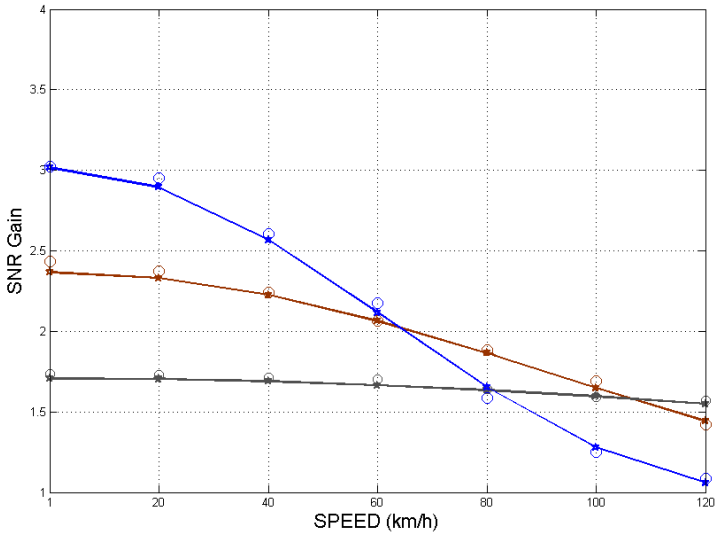

(a) SNR gain vs receiver velocity. Delay = 2 slots.

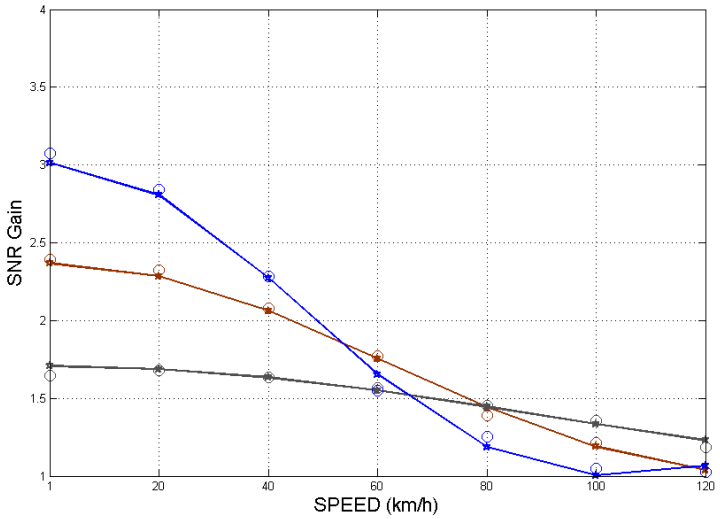

(b) SNR gain vs receiver velocity. Delay = 3 slots.

Figure 5.9: SNR gain with varying number of transmit antennas for quantized cophasing. The simulated values ($\circ$) and the analytical values (solid line, $\star$) are shown for 2 Tx antennas (gray), 3 Tx antennas (brown) and 4 Tx antennas (blue).

Based on the obtained results, it is also possible to design a scheme with clear transition points to choose the different methods, based on the user profile and

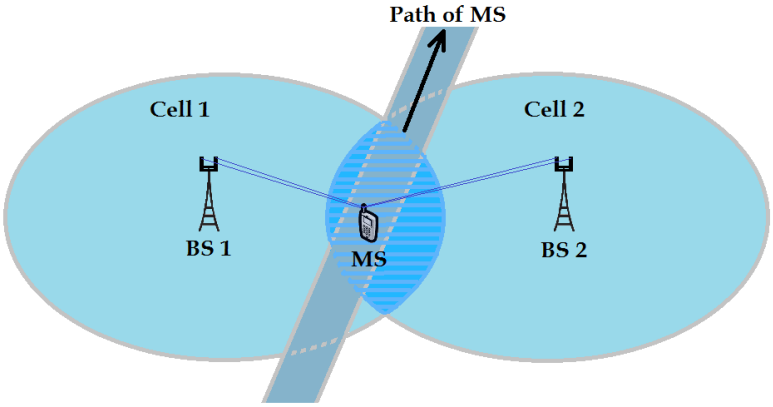

Figure 5.10: Example quantized cophasing system. The coordinated transmission area (blue) is shown between 2 cells (cyan). The mobile terminal is moving along the path lying on the intersection of the 2 cells.

Table 5.2: Decision points for 2 slot delay. The resolution and the number of cooperating transmit antennas can be selected, based on the speed of the mobile station, to result in the best SNR gain.

Speed (km/h)	Resolution	Cooperating Tx Antennas
<40	3	4
40-60	2	4
60-100	2	3
100-120	2	2
>120	1	2

expected feedback delay. Tables 5.2 and 5.3 gives example transition points based on the speed of the receiver, for a delay of 2 slots and 3 slots, respectively.

After the analysis of quantized cophasing in different environments, more scenarios of feedback were considered with the combination of several transmit beamforming techniques. There methods are collectively referred to as hierarchical feedback methods.
The hierarchical methods considered in this Thesis represent a combination of transmit beamforming techniques like TAS and quantized cophasing. The

Table 5.3: Decision points for 3 slot delay. The resolution and the number of cooperating transmit antennas can be selected, based on the speed of the mobile terminal, to result in the best SNR gain.

Speed (km/h)	Resolution	Cooperating Tx Antennas
<20	3	4
40	2	4
60	2	3
>80	1	2

system model and the performance of the hierarchical methods are discussed in the next chapter.

Chapter 6

Simulation of Hierarchical Methods

In the previous chapter, TAS and quantized cophasing were analyzed in detail, and their performances were studied using analytical derivations and simulations. The performance of quantized cophasing was also studied in the case of both, varying feedback resolutions and number of transmit antennas. These methods can be extended to include combinations of the different TBF methods, and it can be verified if these combined methods would be more advantageous for implementation. In this chapter, the different combinations of the TBF techniques are considered, and the methods are collectively called hierarchical methods, and their performance is assessed with the aid of numerical simulations.

6.1 Hierarchical Feedback Method 1

A system model of the proposed hierarchical feedback method 1, henceforth, referred to as hierarchical cophasing-cophasing (HCC), is shown in Fig. 6.1. As can be seen from the figure, the cophasing in this method is done in a hierarchical manner. In the first step, the individual transmitting antennas of a BS are cophased. After this cophasing is performed, the base station signals are cophased.

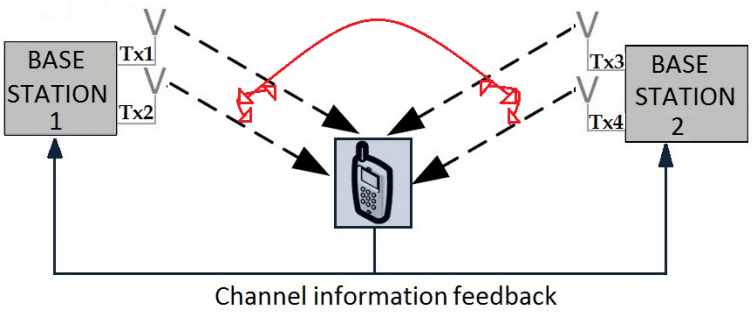

Figure 6.1: Hierarchical cophasing-cophasing. The downlink transmission (black dashed lines) and the uplink feedback signalling (solid black line) is shown. The red lines that indicate the cophasing pairs that are considered in this method.

The use of this method is advantageous from the implementation point of view, as there could be base stations where cophasing between the transmitters already exist, and the upgradation to HCC would involve just the introduction of the signalling required to cophase 2 BSs. Depending on the environment, the resolution of the bits used to cophase the BSs could be changed to optimize the performance, and the option to select the feedback resolution between the different entities is its main advantage over quantized cophasing.

The option to select the feedback resolution is equivalent to having a dynamic number of cooperating base stations, which results in the flexibility of codebook design [34]. Having a flexible feedback weight quantization set would enable the use of the same codebook, regardless of the number of cooperating base stations.

6.2 Hierarchical Feedback Method 2

A system model of the proposed hierarchical method 2, henceforth referred to as hierarchical cophasing-selection (HCS), is shown in the Fig. 6.2. This hierarchical method is a combination of TAS and quantized cophasing, where cophasing is applied between the different transmitters of the BS, and TAS is applied between the base stations. In other words, the base station with the

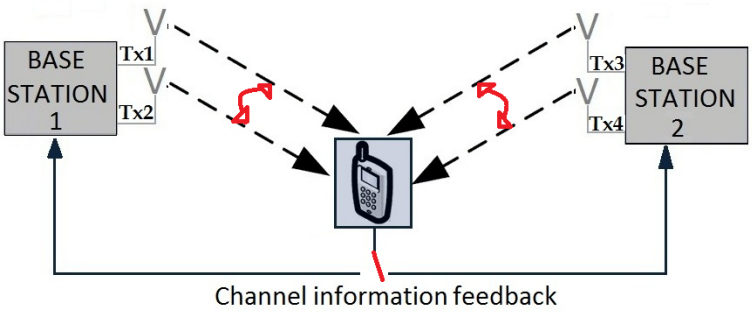

Figure 6.2: Hierarchical Cophasing-Selection. The downlink transmission (black dashed lines) and the uplink feedback signalling (solid black line) is shown. The red lines that indicate the cophasing between transmitters and selection between base stations.

best perceived signal quality is selected.

At the first glance, this method seems to have the least diversity gain as there is only one BS that is serving the MS at any point in time. This, however, can be considered as an advantage in scenarios with high channel power imbalance conditions. In this method, the received signal is only from the strongest BS, as the user does not consider the signal from the base station with weak mean power.

This method is also beneficial to design a flexible codebook that can be used regardless of the number of cooperating BSs. The implementation of this method is relatively simple, as there is cophasing applied in only one step of the hierarchical signalling.

6.3 Performance of Hierarchical Schemes

In this section, the performance of HCC and HCS is assessed based on numerical simulations, and it is compared with the performance of quantized cophasing with 4 transmit antennas. The feedback delay assumed in all the methods is considered identical. It is considered that the delay is the time between the instant when the channel is estimated, and the instant when the

weights are effectively applied in transmission, according to channel estimation.

With the assumption of delay, it could be seen there cannot be direct comparison between quantized cophasing and HCC. It is assumed that the receiver has no intelligence to predict the resulting cophased signal, in order to send the feedback information to cophase the base stations. The lack of prediction causes an inherent extra delay, due to the 2 stages of feedback.

The plot showing the performance of the different systems is shown in Fig. 6.3. As seen from the figure, quantized cophasing has the best performance in the presence of 4 transmit antennas and low power imbalance. It can be assumed to be the upper limit for the SNR gain of a 4 antenna systems considered in this Thesis.

With the increase in channel power imbalance, it can be seen that the HCS method performs much better than the other 2 methods. The improved performance can be attributed to the fact that only the best BS is selected, and the influence of the weak signals to the resultant is eliminated. The performance of the 3 methods in the case of high power imbalance conditions is shown in Fig. 6.4.

Since the comparison of quantized cophasing with HCC could be argued to be unfair, due to the presence of an inherent delay resulting from the hierarchical feedback, another scenario is considered. In this new scenario, an assumption is made, in which it is considered that the receiver can calculate the resulting transmitter cophased signal and predict the BS cophasing weights. As the receiver already has the channel information of the different signals received, with extra processing, it could be assumed that the receiver is able to generate the BS cophasing weights. With this assumption, the simulations were performed, and the results are as shown in Fig. 6.5 for a delay of 2 slots.

From the figures, it is possible to observe that if the base station cophasing feedback information is sent along with the transmitter cophasing feedback

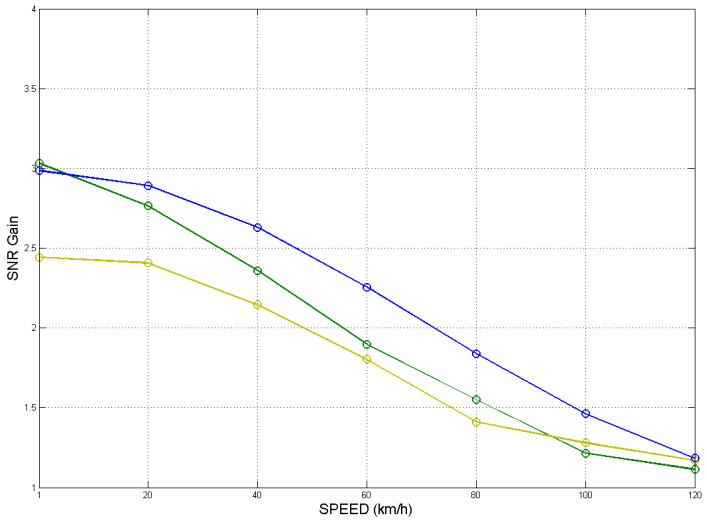

(a) SNR Gain vs Receiver velocity. Delay = 2 slots.

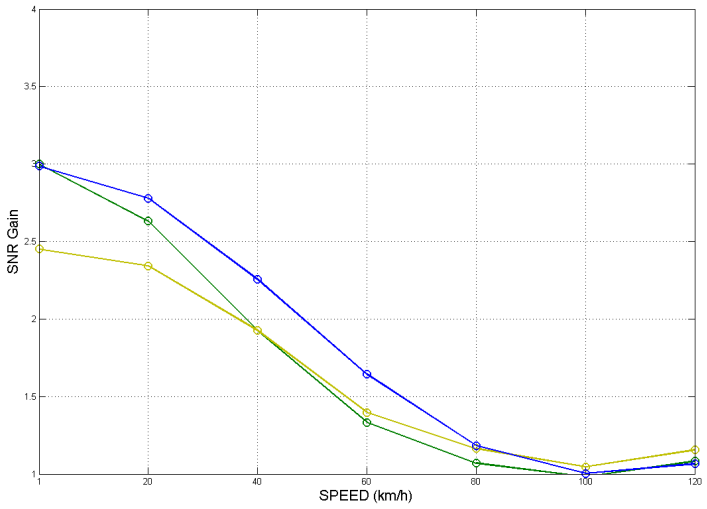

(b) SNR Gain vs Receiver velocity. Delay = 3 slots.

Figure 6.3: SNR gain of hierarchical methods. The numerical simulation results of HCC (green), HCS (yellow) and quantized cophasing (blue) is shown for different values of feedback delay at a low power imbalance of 5 dB.

information, the performance of the HCC system can be improved beyond the performance of quantized cophasing because of the lesser delays involved due to prediction. This is possible as the receiver possesses the channel gains of

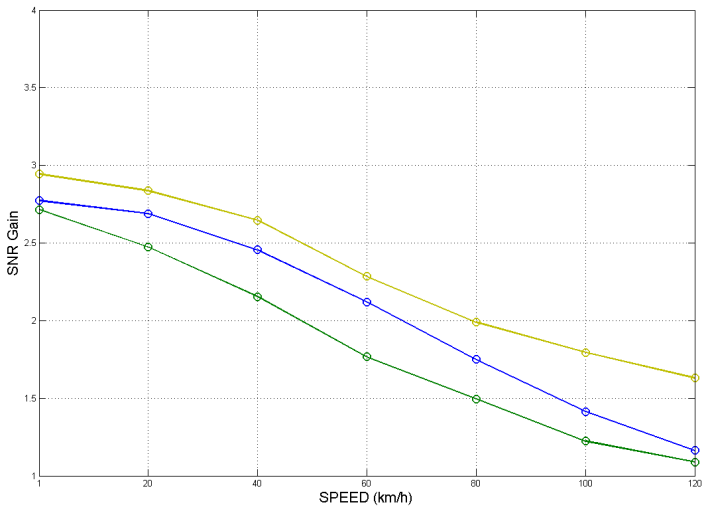

(a) SNR Gain vs Receiver velocity. Delay = 2 slots.

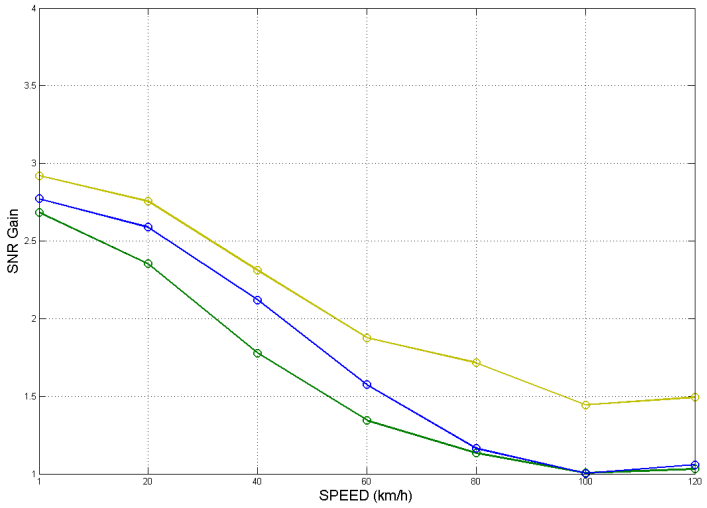

(b) SNR Gain vs Receiver velocity. Delay = 3 slots.

Figure 6.4: SNR gain of hierarchical methods. The numerical simulation results of HCC (green), HCS (yellow) and quantized cophasing (blue) is shown for different values of feedback delay at a high power imbalance of 15 dB.

the received signals. The method would, however, necessitate the shift of processing from the base station to the receiver. This is not particularly feasible, and the implementation issues could prevent its deployment. In this Thesis,

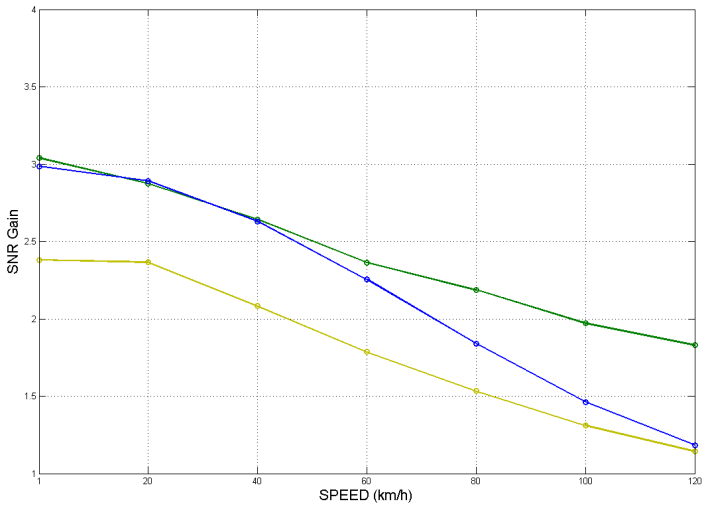

(a) SNR Gain vs Receiver velocity at low imbalance

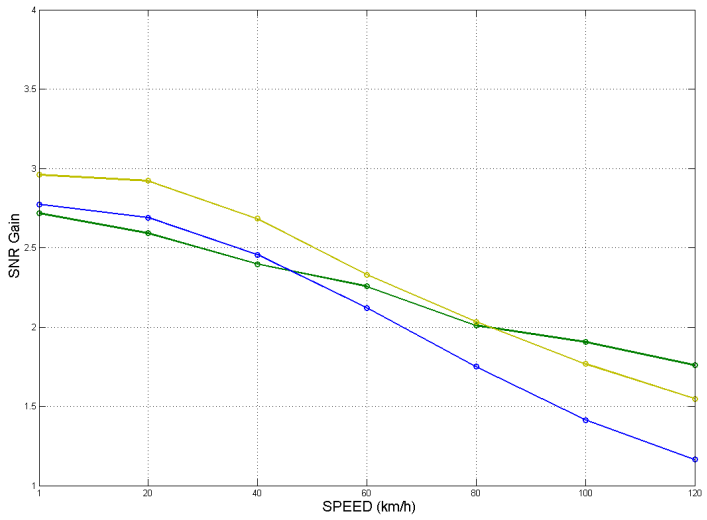

(b) SNR Gain vs Receiver velocity at high imbalance

Figure 6.5: SNR gain of hierarchical methods with intelligent receiver. The numerical simulation results of HCC (green), HCS (yellow) and quantized cophasing (blue) is shown for a delay of 2 slots.

the method is just shown to gauge the performance of the system with an intelligent receiver.

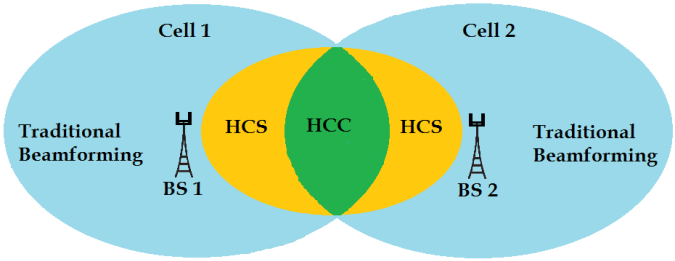

Figure 6.6: Example system with transition points for hierarchical method selection. Based on the power imbalance situation, quantized cophasing or HCC can be used in low power imbalance locations (green), HCS can be used in the high power imbalance locations(yellow).

6.4 Summary

By using all the different results in this chapter, the most preferred method for transmission can be chosen for the given environment. Based on the channel power imbalance conditions, the transition points where the different hierarchical methods could be selected can be defined. An example for the decision points is given in Fig. 6.6.
A brief discussion on the results and the conclusions of this Thesis is given in the next chapter.

Chapter 7

Conclusion

In this chapter, the results of the Thesis are analyzed and the proposal for the most feasible method of transmit diversity is pointed out. The possible future research work in this area is also discussed briefly.

7.1 Inference of the Obtained Results

From the results and plots in chapters 5 and 6, it is evident that the channel conditions play a very important role in the performance of the system, especially when there is feedback delay. In this Thesis, the effect of feedback delay on the system was studied for different transmit diversity methods. It was seen that the performance of the system is good when the number of transmitters used is high, or when there is high feedback resolution, but only at low speeds and delays. The performance of the system deteriorates when the velocity of the MS is increased, or when there is long feedback delay. It is, therefore, necessary to have a balance between the number of transmitters used, and the resolution, to obtain the best SNR gain for a given delay and velocity. From the results of the analysis, an opportunistic feedback mechanism can be conceptualized, where the transmit diversity method is selected dynamically depending on the various parameters.

The different hierarchical systems can also be chosen based on the ease of introduction of new BS signalling messages, and the channel power imbalance

conditions. The use of hierarchical systems result in a flexible codebook design, which further has several implementation advantages. The simulation of performance of the different hierarchical systems were presented. Based on the results, and depending on the power imbalance situation, the transition points between the different methods can be chosen.

7.2 Future Work

The scope and the goals initially defined in the Thesis were all achieved, but the results of the research work could be extended to develop an optimum system. Some of the developments that could be considered are given below.

1. The current work did not make use of any channel prediction algorithms. Channel prediction could be used in the future, and the weights could be adjusted accordingly at the transmitter to alleviate the effect of delay.

2. The Thesis considers a single user, but a system with multiple users could be considered in the downlink. The users could be categorized into groups based on the location and speed, and the user groups could be serviced.

3. The effect of delay could be studied in other hierarchical models that consider the different hierarchical combinations of TBF methods including TAS, quantized cophasing as well as quantized cophasing with order information.

Implementing these steps would result in an optimized system which can be used in multi-user scenarios.

Bibliography

[1] Nokia Siemens Networks, "2020: Beyond 4G. Radio Evolution for the Gigabit Experience." www.nokiasiemensnetworks.com/sites/default/files/document/nokia_siemens_networks_beyond_4g_white_paper_online_20082011_0.pdf, 2011.

[2] Ericsson, "More than 50 billion connected devices." http://www.ericsson.com/res/docs/whitepapers/wp-50-billions.pdf, Feb. 2011.

[3] A. Viterbi, K. Gilhousen, R. Padovani, and I. Wheatley, C., "Universal frequency reuse: the CDMA advantage in capacity for digital cellular radio," in *Conference Proceedings., Tenth Annual International Phoenix Conference on Computers and Communications*, p. 424, Mar. 1991.

[4] K. T. Kim and S. K. Oh, "A universal frequency reuse system in a mobile cellular environment," in *IEEE 65th Vehicular Technology Conference*, pp. 2855 –2859, Apr. 2007.

[5] D. Gesbert, S. Hanly, H. Huang, S. Shamai Shitz, O. Simeone, and W. Yu, "Multi-cell MIMO cooperative networks: A new look at interference," *IEEE Journal on Selected Areas in Communications*, vol. 28, pp. 1380 –1408, Dec. 2010.

[6] J. Hamalainen and R. Wichman, "The effect of feedback delay to the closed-loop transmit diversity in FDD WCDMA," in *12th IEEE International Symposium on Personal, Indoor and Mobile Radio Communications*, vol. 1, pp. D–27 –D–31 vol.1, Sep. 2001.

[7] H. Sun, J. Wang, Y. Wang, and X. You, "Performance analysis of TAS-based MISO system in temporally-correlated channel," in *IEEE 18th International Symposium on Personal, Indoor and Mobile Radio Communications (PIMRC)*, pp. 1 –4, Sept. 2007.

[8] 3GPP, "Evolved Universal Terrestrial Radio Access (E-UTRA); Further advancements for E-UTRA physical layer aspects," TS 36.814, 3rd Generation Partnership Project (3GPP), 2010.

[9] 3GPP, "Coordinated multi-point operation for LTE physical layer aspects," TS 36.819, 3rd Generation Partnership Project (3GPP), 2011.

[10] D. Lee, H. Seo, B. Clerckx, E. Hardouin, D. Mazzarese, S. Nagata, and K. Sayana, "Coordinated multipoint transmission and reception in LTE-advanced: deployment scenarios and operational challenges," *Communications Magazine, IEEE*, vol. 50, pp. 148 –155, Feb. 2012.

[11] L. Qiang, Y. Yang, F. Shu, and W. Gang, "Coordinated beamforming in downlink CoMP transmission system," in *5th International ICST Conference on Communications and Networking in China (CHINACOM)*, pp. 1 –5, Aug. 2010.

[12] S. Das, H. Viswanathan, and G. Rittenhouse, "Dynamic load balancing through coordinated scheduling in packet data systems," in *22nd Annual Joint Conference of the IEEE Computer and Communications (INFOCOM)*, vol. 1, pp. 786 – 796 vol.1, Apr. 2003.

[13] A. Dowhuszko, M. Husso, J. Li, J. Hamalainen, and Z. Zheng, "Performance of practical transmit beamforming methods for interference suppression in closed-access femtocells," in *Future Network Mobile Summit (FutureNetw)*, pp. 1 –12, Jun. 2011.

[14] C. Komninakis, C. Fragouli, A. Sayed, and R. Wesel, "Multi-input multi-output fading channel tracking and equalization using kalman estimation," *IEEE Transactions on Signal Processing*, vol. 50, pp. 1065 –1076, May 2002.

[15] J. Cavers, "An analysis of pilot symbol assisted modulation for rayleigh fading channels [mobile radio]," *IEEE Transactions on Vehicular Technology*, vol. 40, pp. 686 –693, Nov. 1991.

[16] D. Tse and P. Viswanath, *Fundamentals of Wireless Communication*. England: Cambridge University Press, 2005.

[17] T. Rappaport, *Wireless Communications: Principles and Practice*. Upper Saddle River, NJ, USA: Prentice Hall PTR, 2nd ed., 2001.

[18] R.H.Clarke, "A statistical theory of mobile-radio reception," *Bell Systems Technical Journal*, vol. 47, pp. 957 –1000, 1968.

[19] R. Iqbal, T. Abhayapala, and T. Lamahewa, "Generalised clarke model for mobile-radio reception," *IET Communications*, vol. 3, pp. 644 –654, Apr. 2009.

[20] M. Gans, "A power-spectral theory of propagation in the mobile-radio environment," *IEEE Transactions on Vehicular Technology*, vol. 21, pp. 27 – 38, Feb. 1972.

[21] W. C. Jakes, *Microwave Mobile Communications*. Wiley-IEEE Press, 1st ed., 1974.

[22] G. L. Stüber, *Principles of Mobile Communications*. Kluwer Academic Publishers, 2nd ed., 2002.

[23] A. Hottinen, R. Wichman, and O. Tirkkonen, *Multi-Antenna Transceiver Techniques for 3G and Beyond*. New York, NY, USA: John Wiley & Sons, Inc., 2003.

[24] J. Kurjenniemi, J. Leino, Y. Kaipainen, and T. Ristaniemi, "Closed loop mode 1 transmit diversity with high speed downlink packet access," in *International Conference on Communication Technology Proceedings*, vol. 2, pp. 757 – 761 vol.2, Apr. 2003.

[25] 3GPP, "Physical layer procedures (FDD)," TS 25.214, 3rd Generation Partnership Project (3GPP), 2012.

[26] S. Alamouti, "A simple transmit diversity technique for wireless communications," *IEEE Journal on Selected Areas in Communications*, vol. 16, pp. 1451 –1458, Oct. 1998.

[27] J. Hamalainen and R. Wichman, "Closed-loop transmit diversity for FDD WCDMA systems," in *Conference Record of the Thirty-Fourth Asilomar Conference on Signals, Systems and Computers*, vol. 1, pp. 111 –115 vol.1, Nov. 2000.

[28] H. Holma and A. Toskala, *LTE for UMTS: Evolution to LTE-Advanced*. John Wiley & Sons, 2010.

[29] J. Platz, "Downlink transmit diversity for UMTS FDD," Master's thesis, Institüt für Nachrichtentechnik und Hochfrequenztechnik der Technischen Universität Wien, Vienna, Dec. 2001.

[30] J. Hamalainen and R. Wichman, "Asymptotic bit error probabilities of some closed-loop transmit diversity schemes," in *IEEE Global Telecommunications Conference (GLOBECOM)*, vol. 1, pp. 360 – 364 vol.1, Nov. 2002.

[31] J. Hamalainen, *Performance Analysis of Multi-Antenna and Multi-User Methods for 3G and Beyond*. PhD thesis, Helsinki University of Technology, 2007. ISBN 9789512285358.

[32] A. Haghighat, Z. Lin, and G. Zhang, "Haar compression for efficient CQI feedback signaling in 3GPP LTE systems," in *IEEE Wireless Communications and Networking Conference (WNWC)*, pp. 819 –823, Apr. 2008.

[33] E. Bjornson, D. Hammarwall, and B. Ottersten, "Exploiting quantized channel norm feedback through conditional statistics in arbitrarily correlated MIMO systems," *IEEE Transactions on Signal Processing*, vol. 57, pp. 4027 –4041, Oct. 2009.

[34] Y. Cheng, V. Lau, and Y. Long, "A scalable limited feedback design for network MIMO using per-cell product codebook," *IEEE Transactions on Wireless Communications*, vol. 9, pp. 3093 –3099, Oct. 2010.